Quantum quenches and driven dynamics in a single-molecule device

Yuval Vinkler,[1] Avraham Schiller,[1] and Natan Andrei[2]
[1] *Racah Institute of Physics, The Hebrew University, Jerusalem 91904, Israel*
[2] *Center for Materials Theory, Department of Physics, Rutgers University, Piscataway, NJ 08854-8019 USA*

The nonequilibrium dynamics of molecular devices is studied in the framework of a generic model for single-molecule transistors: a resonant level coupled by displacement to a single vibrational mode. In the limit of a broad level and in the vicinity of the resonance, the model can be controllably reduced to a form quadratic in bosonic operators, which in turn is exactly solvable. The response of the system to a broad class of sudden quenches and ac drives is thus computed in a nonperturbative manner, providing an asymptotically exact solution in the limit of weak electron-phonon coupling. From the analytic solution we are able to (1) explicitly show that the system thermalizes following a local quantum quench, (2) analyze in detail the time scales involved, (3) show that the relaxation time in response to a quantum quench depends on the observable in question, and (4) reveal how the amplitude of long-time oscillations evolves as the frequency of an ac drive is tuned across the resonance frequency. Explicit analytical expressions are given for all physical quantities and all nonequilibrium scenarios under study.

PACS numbers: 73.63.b, 71.38.k, 85.65.+h

I. INTRODUCTION

The description of strong electronic correlations far from thermal equilibrium constitutes one of the major open questions of modern condensed matter physics. Even under the most favorable conditions of nonequilibrium steady state, many of the concepts and techniques that have proven so successful in equilibrium are simply inadequate. Recent advancements in a broad range of systems, from time-resolved spectroscopies[1,2] to cold atoms[3,4] and driven nanostructures,[5,6] have opened new and exciting possibilities for studying the nonequilibrium dynamics in response to quantum quenches and forcing fields. Depending on the physical context one is interested in questions of both basic and practical nature, such as what are the underlying time scales governing the dynamics, how long is coherence maintained, and whether and how does the system equilibrate at long times. Some questions, e.g., the issue of equilibration, often require nonperturbative treatments even if the system is tuned to weak coupling.

Recent years have witnessed the development of an array of powerful numerical techniques aimed at tracking the real-time dynamics of interacting low-dimensional systems. In the more specific context of quantum impurity systems these methodologies include time-dependent variants of the density-matrix renormalization group,[7,8] the time-dependent numerical renormalization group,[9,10] different continuous-time Monte Carlo approaches,[11–14] and sparse polynomial space representations.[15] Despite notable successes, part of these methods are subject to finite-size effects and discretization errors, while others are confined to rather short time scales. Analytical efforts in this realm have focused mainly on suitable adaptations of perturbative renormalization-group[16,17] and flow-equation[18] ideas, which in turn neglect higher order terms. Exact analytical solutions, when available, are thus invaluable both for setting a benchmark and for gaining unbiased understanding of the underlying physics. Unfortunately such exact solutions are restricted at present to very special models whose coupling constants must be carefully tuned.[19,20]

In this paper we present an asymptotically exact solution for the nonequilibrium dynamics of a single-molecule transistor in response to various quantum quenches and ac drives. Single-molecule devices have attracted considerable interest lately due to the technological promise of molecular electronics.[21] From a basic-science perspective they offer an outstanding platform to study the electron-phonon coupling at the nano-scale. In a typical molecular bridge, molecular orbitals are coupled simultaneously to the lead electrons and to the vibrational modes of the molecule, with the former degrees of freedom reduced to a single effective band in the absence of a bias voltage.[22] A minimal model for an unbiased molecular bridge therefore consists of a single resonant level coupled by displacement to a single vibrational mode, as described by the Hamiltonian of Eqs. (1) and (2) below.

The spinless Hamiltonian of Eqs. (1) and (2) has been extensively used in recent years to model single-molecule transistors, however despite its apparent simplicity it lacks a complete solution. Conventionally the model is treated either using perturbation theory in the electron-phonon coupling when the coupling is sufficiently weak, or using the Lang-Firsov transformation[23] and the polaronic approximation in the limit where tunneling is sufficiently small. A particularly elegant nonperturbative solution of the model was recently devised by Dóra and Halbritter,[24] who noticed that the original electronic Hamiltonian of Eqs. (1) and (2) can be mapped onto an exactly solvable bosonic form in the limit where the electronic level is broad. Building on prior results[25,26] for the related single-impurity Holstein model, these authors proceeded to compute the temperature-dependent

conductance of the device under strict resonance conditions. Since mapping onto the exactly solvable model is controlled by the smallness of the electron-phonon coupling g as compared to the level width Γ, these results are expected to be asymptotically exact in the weak-coupling limit.

In this paper we take the solution one step further by extending it to the nonequilibrium dynamics in response to a broad class of quantum quenches and drives. We explicitly show that the system thermalizes following a local quantum quench and analyze in detail the time scales involved. In particular, we find that the relaxation time depends on the observable in question, growing by a factor of two in going from the phonon occupancy to the phonon displacement and the electronic occupancy of the level. This is quite surprising since unlike the Anderson impurity model, where spin and charge generally relax on different time scales,[9] the phonon occupancy and displacement pertain to the same degrees of freedom. A related doubling of frequency occurs in the long-time response of the phonon occupancy to an ac drive. These results, as well as others, are obtained in a fully analytic manner, which is perhaps the most appealing aspect of our solution.

Before proceeding to actual calculations, two technical comments are in order. First, some of the scenarios under consideration in this paper pertain to a level off resonance with the Fermi energy, which necessitates the incorporation of the level energy into the bosonic Hamiltonian. A nonzero energy level breaks particle-hole symmetry, an aspect that is missing in the treatment of Dóra and Halbritter. Below we correct their mapping to properly account for this important point. Second, some of the initial states to be considered will be nonthermal states that cannot be treated using the Keldysh technique. We circumvent this complication by explicitly constructing the single-particle eigenmodes of the bosonic Hamiltonian and using them to propagate the system in time.

The reminder of the paper is organized as follows. In Sec. II we introduce the model and its mapping onto a form quadratic in bosonic operators. The bosonic Hamiltonian is solved in turn in Sec. III by explicitly constructing its single-particle eigenmodes using the scattering-state formalism. Technical details of the solution are relegated to the Appendix. The next three sections are devoted to three different quench scenarios: one, Sec. IV, where the electron-phonon interaction is suddenly switched on, another, Sec. V, where the phonon frequency is abruptly shifted from its initial value, and lastly, Sec VI, the scenario where a sudden change is applied to the electronic level. The case of driven dynamics is addressed in Sec. VII, first in its general form before turning to an explicit discussion of ac drives. Finally, we present our conclusions in Sec. VIII

II. THE MODEL AND ITS MAPPING

The Hamiltonian we consider is one of the common models used to describe a single Coulomb-blockade resonance in molecular devices. It consists of a single spinless electronic level $d^\dagger$ with energy ϵ_d, which is coupled by displacement to a local vibrational mode $b^\dagger$ with frequency ω_0. The level is further coupled to a band of spinless electrons via the hopping matrix element t, as described by the Hamiltonian[27]

$$\mathcal{H} = \mathcal{H}_0 + \epsilon_d \hat{n}_d + \omega_0 b^\dagger b + g\left(b^\dagger + b\right)\left(\hat{n}_d - \frac{1}{2}\right), \quad (1)$$

with $\hat{n}_d = d^\dagger d$ and

$$\mathcal{H}_0 = \sum_k \epsilon_k c_k^\dagger c_k + t\sum_k \left(c_k^\dagger d + d^\dagger c_k\right). \quad (2)$$

Here the combination $\hat{Q} = (b^\dagger + b)/\sqrt{2}$ can be thought of as a dimensionless position operator for the local phonon.

The Hamiltonian defined by Eqs. (1) and (2) has a long history that dates back to the 1970s, when it was proposed as a model for the electron-phonon coupling in mixed-valence compounds.[28] In the modern context of nanostructures it is expected to properly describe the physics of single-molecule devices away from Coulomb-blockade valleys where a single unpaired spin resides on the molecule. Typically the Hamiltonian is treated either in the weak-coupling limit using perturbation theory in g, or using the Lang-Firsov transformation[23] and the polaronic approximation in the limit where t is small. We shall take a different route and present a nonperturbative solution to this model which is asymptotically exact in the limit where $\Gamma \gg \max\{g, |\epsilon_d|, g^2/\omega_0\}$. Our approach is based on the fact that the Hamiltonian of Eqs. (1) and (2) can be controllably reduced in this limit to a form quadratic in bosonic operators which is exactly solvable. As discussed in the introduction, this method was first employed in equilibrium by Dóra and Halbritter.[24] Here we exploit this property of the model to calculate the real-time dynamics following different quantum quenches and also in response to ac drives. Accordingly, our presentation begins with the conversion of the Hamiltonian to a form that is quadratic in bosonic operators, whose solution is detailed in turn in Sec. III.

Technically, the construction of the bosonic Hamiltonian proceeds in two steps (Ref. 24): (i) the conversion to a continuum-limit Hamiltonian and (ii) its subsequent bosonization. Special care is paid to the parametric form of the coupling constants that enter the bosonic Hamiltonian and to the role of the energy level ϵ_d which breaks particle-hole symmetry. The latter energy scale is of particular interest as it can be controlled experimentally using suitable gate voltages. In this respect our derivation exceeds that of Dóra and Halbritter.

A. Conversion to a continuum-limit Hamiltonian

Our first goal is to map the Hamiltonian of Eq. (1) onto a continuum-limit form, where the resonant-level operator $d^\dagger$ is replaced with a suitable field operator. To this end, we first diagonalize the Hamiltonian term $\mathcal{H}_0$ using scattering theory to construct its single-particle eigenmodes. These are conveniently expressed using the Green function of the level

$$G(z) = \left[z - \sum_k \frac{t^2}{z - \epsilon_k} \right]^{-1} \tag{3}$$

and its associated phases

$$\phi_k = \arg\left\{ G(\epsilon_k - i\eta) \right\}, \tag{4}$$

where the limit $\eta \to 0^+$ is implied. Specifically, introducing the properly normalized fermionic operators

$$\begin{aligned} \psi_k^\dagger \;=\; & e^{i\phi_k} c_k^\dagger + t\,|G(\epsilon_k + i\eta)| \\ & \times \left[d^\dagger + \sum_{k'} \frac{t}{\epsilon_k - \epsilon_{k'} + i\eta} c_{k'}^\dagger \right], \end{aligned} \tag{5}$$

the Hamiltonian term $\mathcal{H}_0$ can be shown to take the diagonal form

$$\mathcal{H}_0 = \sum_k \epsilon_k \psi_k^\dagger \psi_k, \tag{6}$$

while $d^\dagger$ acquires the mode expansion

$$d^\dagger = t \sum_k |G(\epsilon_k + i\eta)|\, \psi_k^\dagger. \tag{7}$$

Further converting to the continuous energy-shell operators

$$\tilde{\psi}_\epsilon^\dagger = \frac{1}{\sqrt{\rho(\epsilon)}} \sum_k \delta(\epsilon - \epsilon_k) \psi_k^\dagger \tag{8}$$

where $\rho(\epsilon)$ is the conduction-electron density of states, Eqs. (6) and (7) become

$$\mathcal{H}_0 = \int_{-D}^{D} \epsilon \tilde{\psi}_\epsilon^\dagger \tilde{\psi}_\epsilon d\epsilon \tag{9}$$

and

$$d^\dagger = \int_{-D}^{D} \sqrt{\rho_d(\epsilon)} \tilde{\psi}_\epsilon^\dagger d\epsilon. \tag{10}$$

Here D is the conduction-electron bandwidth and

$$\rho_d(\epsilon) = -\frac{1}{\pi} \mathrm{Im}\left\{ G(\epsilon_k + i\eta) \right\} \tag{11}$$

is the spectral function associated with the Green function of Eq. (3).

Our manipulations thus far were exact, independent of details of the band dispersion ϵ_k. To make further progress we consider hereafter the wide-band limit, where the spectral function of Eq. (11) acquires the Lorentzian form $\pi\rho_d(\epsilon) = \Gamma/(\epsilon_k^2 + \Gamma^2)$ with the hybridization width $\Gamma = \pi\rho(0)t^2$ [$\rho(0)$ is the conduction electrons density of states at the Fermi energy]. Physically, Γ serves as a new high-energy cutoff for the integration in Eq. (10). Since $d^\dagger$ is the only electronic degree of freedom that enters the remaining Hamiltonian terms in Eq. (1), Γ acts as a new effective bandwidth for the electron-phonon coupling. We shall next exploit this observation to further manipulate the Hamiltonian of the system.

The Lorentzian cutoff in Eq. (10) is somewhat inconvenient to deal with. However, its precise form should not play any role in the desired limit $\Gamma \gg \max\{g, |\epsilon_d|, g^2/\omega_0\}$, allowing one to adopt a more convenient cutoff scheme. Indeed, it is useful to replace $\rho_d(\epsilon)$ in Eq. (10) with a rectangular box profile[29] that has the same height at $\epsilon = 0$ and shares the same characteristic width:

$$\rho_d(\epsilon) \to \frac{1}{\pi\Gamma} \theta(D_d - |\epsilon|) \tag{12}$$

with

$$D_d = \frac{\pi\Gamma}{2}. \tag{13}$$

Substituting $\rho_d(\epsilon)$ with the box profile of Eq. (12), the full Hamiltonian of Eq. (1) becomes

$$\begin{aligned} \mathcal{H} \;=\; & \int_{-D}^{D} \epsilon \tilde{\psi}_\epsilon^\dagger \tilde{\psi}_\epsilon d\epsilon + \omega_0 b^\dagger b \\ & + \left[\frac{\epsilon_d}{\pi\Gamma} + \frac{g}{\pi\Gamma} \left(b^\dagger + b \right) \right] \int_{-D_d}^{D_d} d\epsilon \int_{-D_d}^{D_d} d\epsilon' : \tilde{\psi}_\epsilon^\dagger \tilde{\psi}_{\epsilon'} :, \end{aligned} \tag{14}$$

where $: \tilde{\psi}_\epsilon^\dagger \tilde{\psi}_{\epsilon'} : = \tilde{\psi}_\epsilon^\dagger \tilde{\psi}_{\epsilon'} - \delta(\epsilon - \epsilon')\theta(-\epsilon)$ stands for normal ordering with respect to the filled Fermi sea. Note that all electronic modes with $|\epsilon| > D_d$ are decoupled from the phonon in Eq. (14) and can therefore be omitted. This amounts to setting $D \to D_d$ in the integration boundaries of the free kinetic-energy term.

The conversion to a continuum-limit Hamiltonian is completed by defining the right-moving field

$$\psi^\dagger(x) = \frac{1}{\sqrt{2aD_d}} \int_{-D_d}^{D_d} e^{-i\epsilon x/v_F} \tilde{\psi}_\epsilon^\dagger d\epsilon, \tag{15}$$

where v_F is the Fermi velocity and

$$a = \frac{\pi v_F}{D_d} = \frac{2v_F}{\Gamma} \tag{16}$$

is a new short-distance cutoff corresponding to a lattice spacing. The new cutoff is connected to the momentum cutoff $k_c = v_F/D_d$ through the standard relation $k_c = \pi/a$. The field operators so defined obey canonical anticommutation relations $\{\psi(x), \psi^\dagger(y)\} = \delta(x-y)$, subject to the regularization $\delta(0) = 1/a$. Recalling that the

local fermion $d^\dagger$ has been mapped in this process onto $\sqrt{a}\psi^\dagger(0)$, this regularization guarantees that $\{d, d^\dagger\} = 1$ is preserved. Written in terms of the new field operators, the Hamiltonian of the system takes the continuum-limit form

$$\begin{aligned}\mathcal{H} \;=\; & -iv_F \int_{-\infty}^{\infty} \psi^\dagger(x)\partial_x\psi(x)dx + \omega_0 b^\dagger b \\ & + \left[\tilde{\epsilon}_d + \lambda\left(b^\dagger + b\right)\right] : \psi^\dagger(0)\psi(0) :\end{aligned} \tag{17}$$

with

$$\lambda \;=\; ga = 2\frac{v_F}{\Gamma}g, \tag{18}$$

$$\tilde{\epsilon}_d \;=\; \epsilon_d a = 2\frac{v_F}{\Gamma}\epsilon_d. \tag{19}$$

Hence, the resonance width Γ, the electron-phonon coupling g, and the energy level ϵ_d have been reduced to two parameters only, which have the dimension of energy times length. It should be stressed that the original conduction-electron bandwidth D has been replaced in Eq. (17) with $D_d \sim \Gamma$, which serves as the new high-energy cutoff for the continuum-limit Hamiltonian.

The Hamiltonian of Eq. (17), first derived in this context by Dóra and Halbritter,[24] is by no means new. It describes the coupling of a localized phonon mode to a conduction band, and as such has been applied in different variants to a broad class of physical systems. For example, Gadzuk considered it as a general impurity model[30] before applying it to the vibrational line shape of diatomic adsorbates on metallic clusters.[31] Yu and Anderson[32] proposed a closely related two-band Hamiltonian as a model for the anomalous properties of A15 materials, while Dóra and Gulácsi[26] used this Hamiltonian to study the inelastic scattering from local vibrational modes. Although the model in its general form lacks a full solution, it can be conveniently handled in the parameter regime of interest to us using the methodology of Abelian bosonization.

B. Abelian bosonization

Our next step is to bosonize the continuum-limit Hamiltonian defined by Eq. (17). Using the standard prescriptions of Abelian bosonization,[33] the fermionic field operator $\psi(x)$ is written as

$$\psi(x) = \frac{1}{\sqrt{2a}} e^{-i\phi(x)}, \tag{20}$$

where the bosonic field $\phi(x)$ has the mode expansion

$$\phi(x) = 2\pi i \sum_{q>0} \frac{\xi_q}{q}\left(a_q e^{iqx} - a_q^\dagger e^{-iqx}\right) - \frac{2\pi x}{L} : \hat{N} : + \hat{\theta}. \tag{21}$$

Here, a_q and $a_q^\dagger$ are canonical bosonic creation and annihilation operators corresponding to the Fourier components of the electronic density, $\hat{N}$ is the total fermionic number operator, $:\hat{O}:$ stands for normal ordering with respect to the filled Fermi sea, and $\hat{\theta}$ is a phase operator conjugate to $\hat{N}$. The coefficients ξ_q have the explicit form

$$\xi_q = \sqrt{\frac{q}{2\pi L}}\, e^{-aq/2\pi}, \tag{22}$$

which includes a suitable ultraviolet momentum cutoff $k_c = \pi/a$.

The rules of bosonization enable one to represent fermionic operators in terms of bosonic ones with an important caveat: the bosonized form of the interaction term is generally not known away from weak coupling. This uncertainty is removed in the limit of interest $\Gamma \gg \max\{g, |\epsilon_d|, g^2/\omega_0\}$, when the standard substitution $: \psi^\dagger(x)\psi(x) := (-1/2\pi)\partial_x\phi(x)$ applies. Restricting attention to this regime, the bosonized Hamiltonian is thus recast as[34]

$$\begin{aligned}\mathcal{H} \;=\; & \sum_{k>0} \epsilon_k a_k^\dagger a_k + \omega_0 b^\dagger b \\ & + \left[\lambda(b^\dagger + b) + \tilde{\epsilon}_d\right] \sum_{q>0} \xi_q \left(a_q + a_q^\dagger\right).\end{aligned} \tag{23}$$

Another important identity pertains to the occupancy of the localized electronic level $\hat{n}_d = d^\dagger d$. Since $d^\dagger$ has been mapped in the continuum limit onto $\sqrt{a}\psi^\dagger(0)$, then $\hat{n}_d - 1/2$ corresponds to $a : \psi^\dagger(0)\psi(0) :$, where we have made use of the fact that the expectation value of $\psi^\dagger(0)\psi(0)$ with respect to the unperturbed Fermi sea is $1/(2a)$ [see Eq. (15) with $x = 0$]. Accordingly, $\hat{n}_d - 1/2$ has the bosonized representation[34]

$$\hat{n}_d - \frac{1}{2} = a \sum_{k>0} \xi_k (a_k^\dagger + a_k). \tag{24}$$

This identity will play a key role in our calculations below.

III. EXACT DIAGONALIZATION

The Hamiltonian of Eq. (23) is quadratic in bosonic operators and as a result is exactly solvable. In the following section we construct its single-particle eigenmodes using the scattering-state formalism. Although of similar technical complexity, it is advantageous to first address the case where $\epsilon_d = 0$, and then extend the discussion to nonzero ϵ_d. This will prove beneficial as we shall be interested, among other things, in cases where the level energy is shifted abruptly from $\epsilon_d = 0$ to nonzero ϵ_d. As we shall see, such a scenario requires the conversion between the eigenmodes of the Hamiltonian with and without ϵ_d. In contrast to the Keldysh technique, the expansion in terms of the eigenmodes of the bosonic Hamiltonian will enable us to address cases of practical interest where the system is initially prepared in a nonthermal state. For example, if the phonon initially occupies an excited state. Our approach is therefore more general than the Keldysh technique.

A. Scattering states for $\epsilon_d = 0$

When a free bosonic mode $a_k^\dagger$ impinges upon the local phonon $b^\dagger$, it is scattered into a linear combination of the free bosonic modes and the localized phonon. This process can be described by the scattering states $\alpha_k^\dagger$, which are eigenmodes of the bosonic Hamiltonian obeying suitable boundary conditions of an incoming free particle. The scattering-state operators can be found by solving the Lippmann-Schwinger equation, which takes the operator form

$$[\alpha_k^\dagger, \mathcal{H}] = -\epsilon_k \alpha_k^\dagger + i\eta(a_k^\dagger - \alpha_k^\dagger). \tag{25}$$

The role of $\eta \to 0^+$ in Eq. (25) is to guarantee appropriate boundary conditions. It does not enter any physical quantities.

A detailed solution of Eq. (25) is presented in Appendix A, using the methodology developed in Ref. 35. Here we quote only the end result. The scattering-state operators are given by

$$\begin{aligned}\alpha_k^\dagger \;=\; & a_k^\dagger + \lambda g(\epsilon_k + i\eta)\xi_k \Big[(\epsilon_k - \omega_0)b + (\epsilon_k + \omega_0)b^\dagger \\ & +\; 2\omega_0 \lambda \sum_{q>0} \xi_q \left(\frac{a_q^\dagger}{\epsilon_k + i\eta - \epsilon_q} + \frac{a_q}{\epsilon_k + i\eta + \epsilon_q} \right) \Big], \end{aligned} \tag{26}$$

where

$$g(z) = \frac{1}{z^2 - \omega_0^2 - 2\omega_0 \Sigma(z)} \tag{27}$$

is related to the phononic Green function of Eq. (A20) and

$$\Sigma(z) = \lambda^2 \sum_{k>0} \xi_k^2 \left(\frac{1}{z - \epsilon_k} - \frac{1}{z + \epsilon_k} \right) \tag{28}$$

is the corresponding self-energy. Both $\Sigma(z)$ and $g(z)$ are analytic in the upper and lower halves of the complex plane, have a branch cut along the real axis, and are even functions of z [i.e., $g(z) = g(-z)$ and likewise for $\Sigma(z)$]. In addition $g(z^*) = g^*(z)$ and $\Sigma(z^*) = \Sigma^*(z)$. These analytical properties are useful in establishing some of the operator identities that will be employed in this paper. In particular, it can be explicitly shown that, in the limit where $L \to \infty$, $\eta \to 0^+$ and yet $L\eta \to \infty$, the Hamiltonian takes the diagonal form

$$\mathcal{H} = \sum_{k>0} \epsilon_k \alpha_k^\dagger \alpha_k, \tag{29}$$

while the scattering-state operators maintain canonical commutation relations:

$$[\alpha_k, \alpha_q^\dagger] = \delta_{k,q}, \tag{30}$$

$$[\alpha_k, \alpha_q] = 0. \tag{31}$$

In fact, the latter commutation relations apply to any finite η, though only the limit $\eta \to 0^+$ is of interest to us.

One particularly useful identity is the expansion of the local phonon mode $b^\dagger$ in terms of the scattering-state operators:

$$\begin{aligned} b^\dagger \;=\; & \lambda \sum_{k>0} \xi_k \Big[g(\epsilon_k - i\eta)(\epsilon_k + \omega_0)\alpha_k^\dagger \\ & - g(\epsilon_k + i\eta)(\epsilon_k - \omega_0)\alpha_k \Big]. \end{aligned} \tag{32}$$

Combined with the diagonal form of the Hamiltonian of Eq. (29), one can immediately write down the time evolution of $b^\dagger(t)$ in the Heisenberg representation, which reads

$$\begin{aligned} b^\dagger(t) \;=\; & \lambda \sum_{k>0} \xi_k \Big[g(\epsilon_k - i\eta)(\epsilon_k + \omega_0) e^{i\epsilon_k t} \alpha_k^\dagger \\ & - g(\epsilon_k + i\eta)(\epsilon_k - \omega_0) e^{-i\epsilon_k t} \alpha_k \Big]. \end{aligned} \tag{33}$$

A similar identity applies to the occupancy of the localized electronic level, whose bosonized form has been detailed in Eq. (24). Expanding the right-hand side of Eq. (24) as

$$a \sum_{k>0} \xi_k (\epsilon_k^2 - \omega_0^2) \left[g(\epsilon_k - i\eta)\alpha_k^\dagger + g(\epsilon_k + i\eta)\alpha_k \right], \tag{34}$$

one has that

$$\begin{aligned} \hat{n}_d(t) \;=\; & \frac{1}{2} + a \sum_{k>0} \xi_k (\epsilon_k^2 - \omega_0^2) \Big[g(\epsilon_k - i\eta) e^{i\epsilon_k t} \alpha_k^\dagger \\ & + g(\epsilon_k + i\eta) e^{-i\epsilon_k t} \alpha_k \Big]. \end{aligned} \tag{35}$$

The operator identities listed in Eqs. (33) and (35) are central to our study as they allow one to track the nonequilibrium dynamics of the phonon mode and the level occupancy, respectively. Accordingly, they will be heavily used throughout the paper.

B. Extension to nonzero ϵ_d

As stated above, the inclusion of a nonzero ϵ_d is quite straightforward and does not add to the complexity of computing the scattering-state operators. Since ϵ_d adds a term linear in bosonic operators to the Hamiltonian [see Eq. (23)], the resulting scattering-state operators differ by a simple k-dependent displacement from their $\epsilon_d = 0$ counterparts (see Appendix A for a detailed derivation). Reserving the notation $\alpha_k^\dagger$ for the scattering-state operators when $\epsilon_d = 0$ and denoting the new operators by $\beta_k^\dagger$, the latter are given by

$$\beta_k^\dagger = \alpha_k^\dagger + \tilde{\epsilon}_d \xi_k \frac{\epsilon_k^2 - \omega_0^2}{\epsilon_k + i\eta} g(\epsilon_k + i\eta), \tag{36}$$

where $\tilde{\epsilon}_d$ and $\alpha_k^\dagger$ are specified in Eqs. (19) and (26), respectively. The shift in scattering-state operators carries over to physical observables as well. For example, the the local phonon mode is expanded as

$$b^\dagger = \tilde{b}^\dagger + \frac{\tilde{\epsilon}_d}{\lambda}\omega_0 g(-i\eta)\Sigma(-i\eta), \tag{37}$$

where $\tilde{b}^\dagger$ is given by the same formal expression of Eq. (32), but with $\alpha_k^\dagger$ and α_k replaced with $\beta_k^\dagger$ and β_k, respectively:

$$\tilde{b}^\dagger = \lambda\sum_{k>0}\xi_k\Big[g(\epsilon_k - i\eta)(\epsilon_k+\omega_0)\beta_k^\dagger - g(\epsilon_k+i\eta)(\epsilon_k-\omega_0)\beta_k\Big]. \tag{38}$$

As discussed below [see Eq. (52) with $\xi \to 0$], the self-energy $\Sigma(-i\eta)$ takes the particularly compact form $-g^2/(\pi\Gamma)$, hence Eq. (37) can be rewritten as

$$b^\dagger = \tilde{b}^\dagger + \frac{\epsilon_d}{\pi\Gamma}\frac{g}{\omega_0}\frac{1}{1-2g^2/(\pi\omega_0\Gamma)}, \tag{39}$$

where we have expressed the constant shift in terms of the original model parameters that appear in Eq. (1).

An analogous expansion applies to the occupancy of the localized level, $\hat{n}_d$, which is written as

$$\hat{n}_d = \tilde{n}_d - \frac{a\tilde{\epsilon}_d}{\lambda^2}\omega_0^2 g(-i\eta)\Sigma(-i\eta). \tag{40}$$

Here

$$\tilde{n}_d = \frac{1}{2} + a\sum_{k>0}\xi_k(\epsilon_k^2-\omega_0^2)\Big[g(\epsilon_k-i\eta)\beta_k^\dagger + g(\epsilon_k+i\eta)\beta_k\Big] \tag{41}$$

is the same formal expression of Eq. (35) with the time t set to zero and with $\alpha_k^\dagger$ and α_k replaced by $\beta_k^\dagger$ and β_k, respectively. As with $b^\dagger$, one can exploit the explicit expression for the self-energy $\Sigma(-i\eta)$ to recast $\hat{n}_d$ in the form

$$\hat{n}_d = \tilde{n}_d - \frac{\epsilon_d}{\pi\Gamma}\frac{1}{1-2g^2/(\pi\omega_0\Gamma)}. \tag{42}$$

Note that the displacement of the scattering-state operators and the associated shifts in the expansions of $b^\dagger$ and $\hat{n}_d$ have a simple physical origin: they reflect the breaking of particle-hole symmetry in the original Hamiltonian of Eq. (1) inflicted by a nonzero ϵ_d. This important aspect of ϵ_d is absent in the mapping of Dóra and Halbritter,[24] who accounted for this energy scale by a simple Lorentzian reduction of the coupling constant λ. Some of the results presented in this work would be missed out unless the breaking of particle-hole is properly treated.

Armed with the single-particle eigenmodes of the full Hamiltonian and with the expansions of physical operators in terms of these modes, we are now in position to compute the real-time dynamics of the system in response to various quantum quenches and ac drives. Specifically, we shall consider three quench scenarios: one where the electron-phonon interaction is abruptly switched on, another where the phonon frequency is suddenly shifted from ω_0 to $\omega_0+\delta\omega$, and finally a sudden change in the level energy from $\epsilon_d = 0$ to nonzero ϵ_d. In addition, we shall consider two ac drives — one applied to the local phonon and another applied to the electronic level. Of particular interest are the characteristic time-scales that govern the nonequilibrium dynamics and their dependences on the physical parameters of the system. These aspects will be analyzed in detail below.

IV. SWITCHING ON THE INTERACTION

We begin our discussion with the nonequilibrium dynamics following an abrupt switching on of the electron-phonon interaction g. We consider the following scenario. At time $t < 0$ the system is free of interactions (i.e., $g = 0$), and occupies a state that is a direct product of the electronic ground state (the filled Fermi sea) and an arbitrary phononic state. Typically one is interested in cases where the phonon has either a well-defined occupation number n or resides in a coherent state, though our discussion is not restricted to these particular choices. At time $t = 0$ the electron-phonon interaction is abruptly switched on and the system evolves under the full Hamiltonian $\mathcal{H}$. This acts to entangle the phononic and electronic degrees of freedom, which are no longer independent. We concentrate our discussion on zero temperature, yet the derivation presented below can readily be extended to any finite temperature T of the Fermi sea.

Formally, the time evolution of the expectation value of an observable $\hat{O}$ is given by the standard expression

$$O(t) = \langle\psi_0|U^\dagger(t,0)\hat{O}U(t,0)|\psi_0\rangle, \tag{43}$$

where $|\psi_0\rangle$ is the initial state of the system and $U(t,0)$ is the time-evolution operator. One is therefore interested in the expectation value of $\hat{O}$ in its Heisenberg representation $\hat{O}(t) = U^\dagger(t,0)\hat{O}U(t,0)$ with respect to the initial state $|\psi_0\rangle$. In the scenario under consideration the initial state has a simple representation in terms of the eigenmodes of the initial Hamiltonian with $g = 0$, whereas the time evolution has a natural representation in terms of the eigenmodes of the full (i.e., final) Hamiltonian $\mathcal{H}$. Therefore, the general strategy for calculating $O(t)$ proceeds as follows. First $\hat{O}(t)$ is represented in terms of the eigenmodes of the full Hamiltonian where its time evolution can easily be implemented, next it is recast in terms of the eigenmodes of the initial Hamiltonian, and finally the expectation value with respect to $|\psi_0\rangle$ is evaluated. Below we implement this procedure to track the time evolution of the phononic occupancy $n_b(t) = \langle b^\dagger(t)b(t)\rangle$ and displacement $Q(t) = \frac{1}{\sqrt{2}}\langle b^\dagger(t) + b(t)\rangle$. Throughout the section we set ϵ_d equal to zero, corresponding to a level at resonance with the Fermi energy.

A. Time evolution of phononic operators

Our first goal is to express $b^\dagger(t)$ in terms of a_k, $a_k^\dagger$, b and $b^\dagger$, which are the eigenmodes of the initial Hamiltonian with $g = 0$. The expansion of $b^\dagger(t)$ in terms of the eigenmodes of the final Hamiltonian is detailed in Eq. (33). Substituting the explicit expression for the scattering-state operators, Eq. (26), into Eq. (33) one obtains

$$b^\dagger(t) = \lambda \sum_{k>0} \xi_k \left[F(\epsilon_k - i\eta, t) a_k^\dagger + F(-\epsilon_k - i\eta, t) a_k \right] + I_1(t) b + I_2(t) b^\dagger, \tag{44}$$

where we have introduced three auxiliary functions

$$I_1(t) = \lambda^2 \sum_{k>0} \xi_k^2 \left| g(\epsilon_k + i\eta) \right|^2 (\epsilon_k^2 - \omega_0^2) \left(e^{i\epsilon_k t} - e^{-i\epsilon_k t} \right), \tag{45}$$

$$I_2(t) = \lambda^2 \sum_{k>0} \xi_k^2 \left| g(\epsilon_k + i\eta) \right|^2 \left[(\epsilon_k + \omega_0)^2 e^{i\epsilon_k t} - (\epsilon_k - \omega_0)^2 e^{-i\epsilon_k t} \right], \tag{46}$$

$$F(z,t) = g(z)(z + \omega_0) e^{izt} + 2\omega_0 \lambda^2 \sum_{k>0} \xi_k^2 \left| g(\epsilon_k + i\eta) \right|^2 \left(\frac{\epsilon_k + \omega_0}{\epsilon_k - z} e^{i\epsilon_k t} - \frac{\epsilon_k - \omega_0}{\epsilon_k + z} e^{-i\epsilon_k t} \right). \tag{47}$$

In general, one must resort to numerical integration to accurately evaluate the three functions defined above at arbitrary time t. Results of such numerical calculations will be presented below for the relevant observables of interest. It is instructive, however, to first gain analytical insight by analyzing the long-time behaviors of the auxiliary functions. In the limit $L \to \infty$ one can replace the sums over k with integrals over energy, resulting in an exponential decay at long times of all items but the first term on the right-hand side of Eq. (47). To see this important point consider $I_1(t)$, for example. Converting the sum over k into integration over energy, one is left with the integral

$$I_1(t) = (\rho_0 \lambda)^2 \int_0^\infty d\epsilon \left| g(\epsilon + i\eta) \right|^2 (\epsilon^2 - \omega_0^2) \times \epsilon \left(e^{i\epsilon t} - e^{-i\epsilon t} \right) e^{-\epsilon / D_d}, \tag{48}$$

where $\rho_0 = 1/(2\pi v_F)$ is the density of states per unit length. Focusing on $t \gg 1/D_d$, one may (i) omit the exponential cutoff $e^{-\epsilon/D_d}$ in Eq. (48) and (ii) interchange $\epsilon \to -\epsilon$ in the second term in the parenthesis to obtain

$$I_1(t) \simeq (\rho_0 \lambda)^2 \int_{-\infty}^\infty d\epsilon \left| g(\epsilon + i\eta) \right|^2 \epsilon \, (\epsilon^2 - \omega_0^2) e^{i\epsilon t}. \tag{49}$$

The function $g(\epsilon + i\eta)$ is analytic in the upper half of the complex plane, whereas the analytic continuation of $g^*(\epsilon + i\eta)$ to the upper half plane has a set of isolated poles[36] of the form $p_j = \omega_j + i/\tau_j$ with $\tau_j > 0$. Using these poles one can formally perform the integral in Eq. (49) to arrive at

$$I_1(t) \simeq 2\pi i (\rho_0 \lambda)^2 \sum_j R_j (p_j^2 - \omega_0^2) p_j e^{i\omega_j t - t/\tau_j}, \tag{50}$$

where R_j is the residue of $|g(\epsilon + i\eta)|^2$ at p_j. Thus, for $t \gg 1/D_d$, the function $I_1(t)$ is well approximated by a discrete sum of exponential terms that contain both an oscillatory component and a part that decays in time. Asymptotically only those terms with the largest decay time τ_j dominate, hence $I_1(t)$ closely follows a simple exponential decay with superimposed oscillations. A similar procedure can be applied to $I_2(t)$ and to the term involving the sum over k in the expression for $F(z,t)$, both of which are found to be dominated by the same set of poles p_j provided z lies in the lower half plane (as is the case throughout our calculations).

Next we address the poles p_j, which are given by the solutions to the equation

$$z^2 - \omega_0^2 - 2\omega_0 \Sigma^{(+)}(z) = 0, \tag{51}$$

where $\Sigma^{(+)}(z)$ is the analytic continuation of $\Sigma^*(\epsilon + i\eta)$ to the upper half plane. For $L \to \infty$, the self-energy of Eq. (28) has the explicit analytic expression

$$\Sigma(z) = (\rho_0 \lambda)^2 D_d \left[\xi e^\xi E_1(\xi) - \xi e^{-\xi} E_1(-\xi) - 2 \right], \tag{52}$$

where ξ equals z/D_d and $E_1(z)$ is the Exponential Integral function.[37] Expanding $E_1(z)$ as a logarithm plus a power series in z one obtains $\Sigma^*(\epsilon + i\eta) = (\rho_0\lambda)^2 D_d \left[i\pi\tilde{\epsilon} - 2 + \mathcal{O}\left(\tilde{\epsilon}^2 \ln \tilde{\epsilon}\right) \right]$ with $\tilde{\epsilon} = \epsilon/D_d$, resulting in

$$\Sigma^{(+)}(z) = (\rho_0 \lambda)^2 D_d \left[i\pi\xi - 2 + \mathcal{O}\left(\xi^2 \ln \xi\right) \right]. \tag{53}$$

In general, Eq. (51) lacks an analytical solution. However, in the desired limit where $\rho_0 \lambda = g/(\pi\Gamma) \ll 1$ and $\omega_0 \ll D_d$ one can truncate the expansion of $\Sigma^{(+)}(z)$ at linear order in ξ, to be left with a simple quadratic equation in Eq. (51). In this limit only two poles exist, which

differ in the sign preceding the frequency: $p_\pm = \pm\omega + i/\tau$ with

$$\omega = \omega_0 \sqrt{1 - \frac{2}{\pi}\frac{g^2}{\omega_0 \Gamma} - \frac{1}{\pi^2}\left(\frac{g}{\Gamma}\right)^4}. \tag{54}$$

The decay time τ is given in this approximation by $\tau = \pi\Gamma^2/(\omega_0 g^2)$, where we have converted back to the original model parameters of Eq. (1) in writing both the frequency ω and the single relaxation time τ. Note that these expressions for ω and τ coincide with second-order perturbation theory in g when applied directly to the electronic Hamiltonian of Eq. (1),[38] thus validating the cutoff scheme used in bosonization. The expression for τ can be further improved by going to the next order in ω_0/D_d, i.e., by including one more order in ξ in the expansion of $\Sigma^{(+)}(z)$. This in turn yields

$$\tau = \frac{\pi}{\omega_0}\left(\frac{\Gamma}{g}\right)^2 \left[1 + \frac{2}{\pi}\frac{\omega_0}{\Gamma}\right], \tag{55}$$

where we have restricted ourselves to linear order in ω_0/D_d in writing the expression in the square brackets.

As we shall confirm by explicit numerical calculations, the nonequilibrium dynamics of all observables of interest is governed exclusively by ω and τ at time scales exceeding $1/D_d$. Similar results for ω and $1/\tau$ were reported by Dóra and Halbritter[24] (corresponding in their notation to the real and imaginary parts of $\omega_{p\pm}$), yet their expression for ω contained the bare conduction-electron bandwidth D rather than the renormalized one $D_d \sim \Gamma \ll D$. Indeed, Eqs. (54) and (55) are free of the bandwidth D, indicating that one can safely implement the limit $D \to \infty$ for the Hamiltonian of Eq. (1), provided Γ, g, and ω_0 are all held fixed. Physically this reflects the fact that the local phonon couples to the conduction band by way of the resonant level only, hence its level width Γ serves as a new effective high-energy cutoff. By contrast, there is no meaningful $D_d \to \infty$ limit for the continuum-limit Hamiltonian of Eq. (17) that keeps both ω and τ finite.

Equation (54) features two special values of the electron-phonon coupling g. One, g_0, above which the frequency ω becomes imaginary (i.e., $p_\pm$ become purely imaginary) and another, slightly larger coupling g_c, above which the pole p_- is shifted to the lower half plane. The former coupling strength represents the point where the local phonon is completely softened, whereas the latter value represents the point above which the energy of the lowest bosonic eigenmode of the Hamiltonian of Eq. (23) becomes negative. Both values of g lie well beyond the applicability of our theory, as the mapping onto the continuum-limit Hamiltonian assumed $\Gamma \gg \max\{g, g^2/\omega_0\}$. Interestingly, it has been argued by Dóra[25] that the bosonized Hamiltonian of Eq. (23) offers a faithful representation of the continuum-limit Hamiltonian of Eq. (17) all the way up to strong coupling, where the nonlinear conversion between the fermionic and the bosonic coupling constants is not explicitly known. In particular, the point where p_- is shifted to the lower half plane was identified by Dóra with $\lambda \to \infty$. It remains to be seen whether such strong electron-phonon couplings can indeed be described by a bosonized Hamiltonian with just a simple linear displacement coupling, or whether additional nonlinear terms must be included.

B. Phononic occupancy and displacement

With the explicit expansions of $b^\dagger(t)$ and $b(t)$ at hand we can proceed to compute the time evolution of physical observables, starting with the phonon occupancy $n_b(t)$ and displacement $Q(t)$. Since $b^\dagger(t)$ is linear in the eigenmodes of the initial Hamiltonian, the phonon number operator $\hat{n}_b(t) = b^\dagger(t)b(t)$ is quadratic in these operators. When averaged with respect to the initial state, only the combinations $a_k a_k^\dagger$, $b^\dagger b$, $bb^\dagger$, bb, and $b^\dagger b^\dagger$ contribute to the expectation value of $\hat{n}_b$ at time t, resulting in

$$\begin{aligned} n_b(t) \;=\; & \lambda^2 \sum_{k>0} \xi_k^2 \left|F(-\epsilon_k - i\eta, t)\right|^2 + \left|I_1(t)\right|^2 \left[n_b(0) + 1\right] \\ & + \left|I_2(t)\right|^2 n_b(0) + 2\mathrm{Re}\left\{I_1(t) I_2^*(t) \langle bb\rangle_{t=0}\right\}. \end{aligned} \tag{56}$$

Equation (56) is the central result of this subsection. It provides an asymptotically exact expression for the time evolution of $n_b(t)$ in the weak-coupling regime. Several comments should be made about this result. First, the occupancy $n_b(t)$ depends on the initial state of the phonon via two parameters only: $n_b(0)$ and $\langle bb\rangle_{t=0}$. Any two initial states that share the same values of $n_b(0)$ and $\langle bb\rangle_{t=0}$ will produce identical curves for $n_b(t)$. Second, since $I_1(t)$ and $I_2(t)$ decay to zero with time, the occupancy at long times is independent of the initial state of the phonon. Third, the term involving the summation over k in Eq. (47) decays to zero as well, resulting in a compact expression for the phononic occupancy at long times:

$$n_b(t \to \infty) = \lambda^2 \sum_{k>0} \xi_k^2 \left|g(\epsilon_k + i\eta)\right|^2 (\epsilon_k - \omega_0)^2. \tag{57}$$

Finally, one can show that Eq. (57) is just the zero-temperature equilibrium phonon occupancy with respect to the full Hamiltonian,[39] implying thermalization at long times. This result on its own is not surprising, since it has been rigorously shown by Ambegaokar[40] that Hamiltonians involving a local bosonic mode coupled linearly to a macroscopic bosonic bath do indeed equilibrate at long times in response to a local quantum quench. Below we analyze in detail the decay to the new thermal equilibrium.

Figures 1 and 2 summarize the time evolution of $n_b(t)$, for different coupling constants and different initial conditions. In Fig. 1 we have plotted $n_b(t)$ in response to an abrupt switching on of the electron-phonon coupling g, with the phonon initially occupying the empty state $|0\rangle$ at time $t = 0$. Different values of g are depicted. Starting from $n_b(0) = 0$, the time-dependent occupancy first overshoots its new equilibrium value, to which it then decays

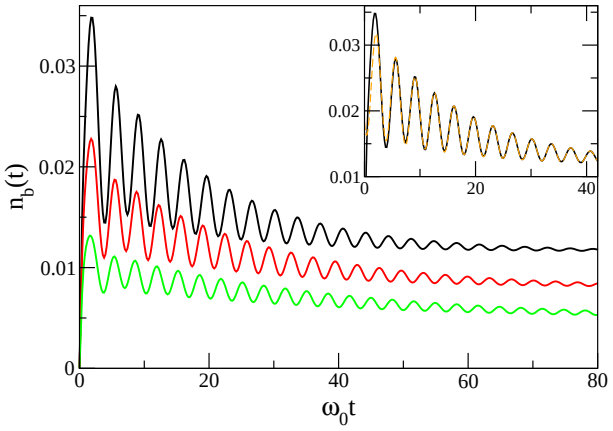

FIG. 1: (Color online) Time evolution of the phonon occupancy $n_b(t)$ following an abrupt switching on of the electron-phonon coupling g at time $t = 0$, with the phonon initially occupying the empty state $|0\rangle$. Here $\omega_0/D_d = 0.2$, while g/Γ equals 0.229 (green), 0.28 (red), and 0.324 (black). The corresponding values of $g^2/(\omega_0\Gamma)$ are 1/6, 1/4, and 1/3, respectively. Inset: A fit of the $g/\Gamma = 0.324$ curve to the functional form of Eq. (58) using the fitting range $9 \leq \omega_0 t \leq 95$. The two curves practically coincide above $\omega_0 t = 8$.

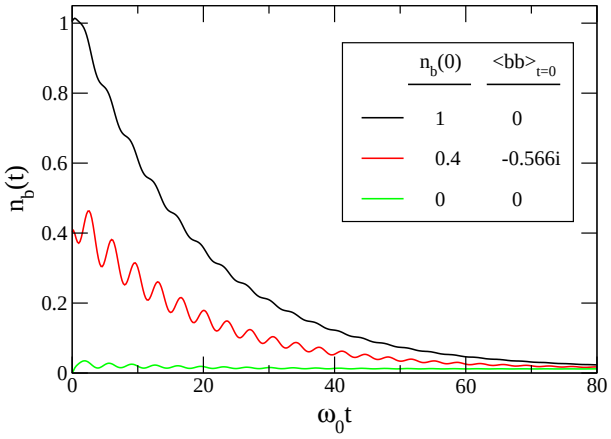

FIG. 2: (Color online) Time evolution of the phonon occupancy $n_b(t)$ following an abrupt switching on of the electron-phonon coupling g, for $g/\Gamma = 0.324$, $\omega_0/D_d = 0.2$, and different initial phononic states. Each of the curves with $n_b(0) > 0$ corresponds to a family of initial states whose values of $n_b(0)$ and $\langle bb\rangle_{t=0}$ are specified in the legends. Representative states for each category are $[2|0\rangle - i|2\rangle]/\sqrt{5}$ (red) and $|1\rangle$ (green). The curve with $n_b(0) = 0$ (black) corresponds exclusively to the initial state $|0\rangle$.

with superimposed oscillations. The oscillatory decay is well described by the long-time behaviors of $I_1(t)$, $I_2(t)$, and the term involving the sum over k in the expression for $F(z,t)$. Indeed, based on our previous analysis one expects $n_b(t \gg 1/D_d)$ to follow the functional form

$$n_b(t) = [A\sin(2\Omega t + \phi) + B]\, e^{-2t/\tau_0} + C, \qquad (58)$$

with Ω and τ_0 equal to ω and τ of Eqs. (54) and (55). The inset of Fig. (1) shows a typical fit of the $g/\Gamma = 0.324$ curve to the functional form of Eq. (58) using the fitting range $9 \leq \omega_0 t \leq 95$. While some deviations are seen at shorter times, the two curves are hardly distinguishable above $\omega_0 t = 8$. Moreover, the extracted values of $\Omega/\omega 0 = 0.896$ and $\tau_0\omega_0 = 35.5$ fall within 1.2% from those of ω and τ quoted above. The agreement between the predicted and extracted parameters is equally good for the two curves with the smaller values of g, confirming our analytic predictions for the long-time behavior of $n_b(t)$.

Figure 2 displays the complementary dependence of $n_b(t)$ on the initial state of the localized phonon. As emphasized above, $n_b(t)$ depends on the initial state of the phonon via two parameters only: $n_b(0)$ and $\langle bb\rangle_{t=0}$. Hence each curve with $n_b(0) > 0$ corresponds to a family of initial states. It is nevertheless useful to have a particular initial state in mind by assigning a representative state to each combination of $n_b(0)$ and $\langle bb\rangle_{t=0}$. One possible choice of states for the two curves with $n_b(0) > 0$ are $[2|0\rangle - i|2\rangle]/\sqrt{5}$ (red line) and $|1\rangle$ (green line). The curve with $n_b(0) = 0$ (black line) corresponds exclusively to $|0\rangle$ as the initial state.

As in Fig. 1, all curves in Fig. 2 can be fit equally well to the functional form of Eq. (58) using the same pair of values for Ω and τ_0 that were extracted for $n_b(0) = 0$. Generally speaking, the larger is $n_b(0)$ the more pronounced is the component of the pure exponential decay, while the magnitude of the superimposed oscillations is more sensitive to $\langle bb\rangle_{t=0}$.

Another quantity of interest is the time evolution of the phonon displacement, $Q(t)$. Since Q is strictly zero for $\epsilon_d = 0$ in thermal equilibrium, its time evolution remains pinned to zero unless either ϵ_d or $\langle b\rangle_{t=0}$ is nonzero. In this section we consider the latter possibility where $\langle b\rangle_{t=0}$ is nonzero. A straightforward evaluation of $Q(t)$ using Eq. (33) and its Hermitian conjugate yields

$$Q(t) = \sqrt{2}\,\mathrm{Re}\big\{[I_1(t) + I_2^*(t)]\langle b\rangle_{t=0}\big\}, \qquad (59)$$

whose dependence on the initial state is reduced to the sole parameter $\langle b\rangle_{t=0}$. Writing the latter in terms of its magnitude and phase, $\langle b\rangle_{t=0} = |\langle b\rangle|e^{i\varphi}$, the time-dependent displacement depends linearly on $|\langle b\rangle|$. The dependence on φ is less transparent as it requires detailed knowledge of $I_1(t)$ and $I_2(t)$. Numerical calculations reveal, however, that the dependence on φ is rather weak, hence we focus our attention hereafter on $\varphi = 0$.

Figure 3 depicts the time evolution of $Q(t)$ for $\langle b\rangle_{t=0} = 1$ and two representative values of the electron-phonon coupling g. As can be seen, $Q(t)$ displays damped oscillations with a frequency and decay time that depend on the magnitude of g. Indeed, based on our previous analysis of $I_1(t)$ and $I_2(t)$ one expects the long-time behavior of $Q(t)$ to follow the functional form

$$Q(t) = A\sin(\Omega t + \phi)e^{-t/\tau_0} \qquad (60)$$

with Ω and τ_0 equal to ω and τ, respectively. Fits to Eq. (60) yield excellent agreement, with values of Ω

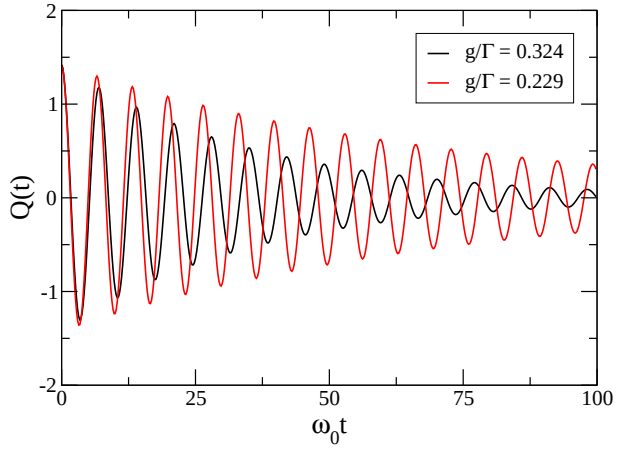

FIG. 3: (Color online) Time evolution of the phonon displacement $Q(t)$, starting from an initial phonon state where $\langle b\rangle_{t=0} = 1$. Here ω_0/D_d equals 0.2. Two representative values of the electron-phonon coupling are depicted: $g/\Gamma = 0.324$ (black) and $g/\Gamma = 0.229$ (red), corresponding to $g^2/(\omega_0\Gamma) = 1/3$ and $1/6$, respectively.

and τ_0 that coincide to within less than 1% with those extracted from Fig. 1 using fits to Eq. (58).[41] Thus, $Q(t)$ displays a relaxation time twice as long as that of $n_b(t)$ and half the frequency of oscillations. Such a relation is quite natural for a classical oscillator where $n_b(t) = \langle b^\dagger(t)\rangle\langle b(t)\rangle \sim Q^2(t)$, but is less obvious for the quantum case considered here.

C. Phononic wave function

Lastly we shall address the time evolution of the phononic wave function, defined as

$$|\psi_{\rm ph}(x,t)|^2 = \langle\delta(\hat{Q}(t) - x)\rangle. \tag{61}$$

Here, $\hat{Q}(t) = U^\dagger(t,0)\hat{Q}U(t,0)$ is the phonon displacement operator in its Heisenberg representation, x is a dimensionless position coordinate, and averaging is taken with respect to the initial state of the system. In thermal equilibrium $|\psi_{\rm ph}(x,t)|^2$ was calculated by Dóra,[25] who showed that it takes a simple Gaussian form. Below we extend the calculation to nonequilibrium quench dynamics, allowing for an arbitrary initial phonon state.

Following Dóra we begin by rewriting Eq. (61) as

$$|\psi_{\rm ph}(x,t)|^2 = \int_{-\infty}^{\infty}\frac{ds}{2\pi}\langle e^{is(\hat{Q}(t)-x)}\rangle. \tag{62}$$

Since $\hat{Q}(t)$ is linear in bosonic operators, and since averaging on the right-hand side is taken with respect to a product state of the filled Fermi sea and the initial phonon state, $\langle e^{is(\hat{Q}(t)-x)}\rangle$ can be recast as the product of two independent averages of the conduction-electron and local-phonon components of $\hat{Q}(t)$. Explicitly, denoting the two components of $\hat{Q}(t)$ by $\hat{Q}_c(t)$ and $\hat{Q}_b(t)$ one has that

$$\langle e^{is\hat{Q}(t)}\rangle = \langle e^{is\hat{Q}_b(t)}\rangle_{\rm b}\langle e^{is\hat{Q}_c(t)}\rangle_{\rm FS}\,, \tag{63}$$

where $\langle\ldots\rangle_{\rm FS}$ and $\langle\ldots\rangle_{\rm b}$ stand for averaging with respect to the filled Fermi sea and the initial phononic state, respectively.

Each of the two averages in Eq. (63) can be evaluated in turn using standard bosonic techniques. Consider first the conduction-electron component. As the average is taken with respect to the ground state of a free bosonic bath one can use the identity $\langle e^{\hat{A}}\rangle = e^{\langle\hat{A}^2\rangle/2}$, applicable to any operator $\hat{A}$ that is linear in bosonic creation and annihilation operators. This results in

$$\langle e^{is\hat{Q}_c(t)}\rangle_{\rm FS} = \exp\left[-\frac{s^2}{2}\langle\hat{Q}_c^2(t)\rangle_{\rm FS}\right]. \tag{64}$$

Moving on to the local phonon component, we first note that $\hat{Q}_b(t)$ has the explicit form

$$\hat{Q}_b(t) = I_3(t)b^\dagger + I_3^*(t)b, \tag{65}$$

where

$$\begin{aligned} I_3(t) &= \frac{1}{\sqrt{2}}\big[I_1^*(t) + I_2(t)\big] = \sqrt{2}\omega_0\lambda^2\sum_{k>0}\xi_k^2|g(\epsilon_k + i\eta)|^2 \\ &\quad\times\left[(\epsilon_k - \omega_0)e^{i\epsilon_k t} + (\epsilon_k + \omega_0)e^{-i\epsilon_k t}\right]. \end{aligned} \tag{66}$$

Next we use the identity $e^{\hat{A}+\hat{B}} = e^{\hat{A}}e^{\hat{B}}e^{[\hat{B},\hat{A}]/2}$, applicable to any two operators $\hat{A}$ and $\hat{B}$ whose commutator is a c-number, to write

$$\langle e^{is\hat{Q}_b(t)}\rangle_{\rm b} = e^{-(s^2/2)|I_3(t)|^2}\langle e^{isI_3(t)b^\dagger}e^{isI_3^*(t)b}\rangle_{\rm b}. \tag{67}$$

The combination of Eqs. (63), (64), and (67) then yields

$$|\psi_{\rm ph}(x,t)|^2 = \int_{-\infty}^{\infty}\frac{ds}{2\pi}e^{-\gamma(t)s^2 - isx}\langle e^{isI_3(t)b^\dagger}e^{isI_3^*(t)b}\rangle_{\rm b} \tag{68}$$

with

$$\gamma(t) = \omega_0^2\lambda^2\sum_{k>0}\xi_k^2\,|K(\epsilon_k - i\eta, t)|^2 + \frac{1}{2}|I_3(t)|^2 \tag{69}$$

and

$$\begin{aligned} K(z,t) &= g(z)e^{izt} + 2\omega_0\lambda^2\sum_{q>0}\xi_q^2|g(\epsilon_q + i\eta)|^2 \\ &\quad\times\left(\frac{e^{i\epsilon_q t}}{\epsilon_q - z} + \frac{e^{-i\epsilon_q t}}{\epsilon_q + z}\right). \end{aligned} \tag{70}$$

Equation (68) allows one to calculate the phononic wave function for arbitrary time $t > 0$ and any initial phononic state. Before turning to concrete examples let us address some generic features of $|\psi_{\rm ph}(x,t)|^2$. Since $I_3(t)$ decays to zero as $t \to \infty$, the expectation value on the right-hand side of Eq. (68) reduces asymptotically to

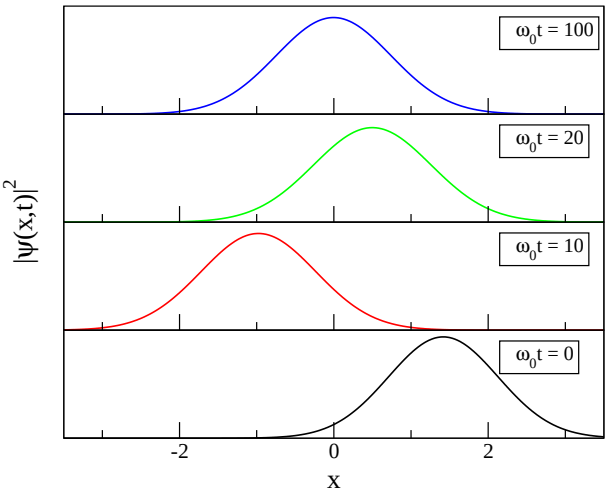

FIG. 4: (Color online) Time evolution of the phononic wave function $|\psi(x,t)|^2$, starting from an initial coherent state with $\lambda = 1$. Here $\omega_0/D_d = 0.2$ and $g/\Gamma = 0.324$.

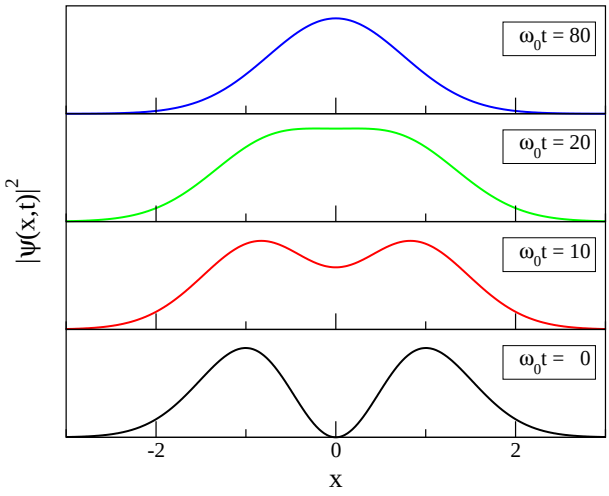

FIG. 5: (Color online) Same as Fig. 4, starting from an initial phonon state where $\hat{n}_b = 1$.

one regardless of the initial state of the phonon. Furthermore, repeating the same type of analysis as beforehand one finds that the term involving the sum over q in the expression for $K(\epsilon_k - i\eta, t)$ decays to zero with the relaxation time τ, and that $\gamma(t)$ decays to its asymptotic value

$$\gamma = \lim_{t\to\infty} \gamma(t) = \lambda^2\omega_0^2 \sum_{k>0} \xi_k^2 \left|g(\epsilon_k + i\eta)\right|^2 \tag{71}$$

with the reduced relaxation time $\tau/2$. The phononic wave function thus takes the asymptotic Gaussian form

$$|\psi_{\rm ph}(x)|^2 = \lim_{t\to\infty} |\psi_{\rm ph}(x,t)|^2 = \frac{1}{2\sqrt{\pi\gamma}} \exp\left[-\frac{x^2}{4\gamma}\right]. \tag{72}$$

Lastly, recognizing that γ is half the thermalized expectation value of $\hat{Q}^2$, i.e., $2\gamma = \langle \hat{Q}^2 \rangle_{\rm eq}$, we recover hereby the equilibrium result of Dóra[25] at long times.

While the asymptotic form of the phononic wave function is independent of the initial state of the phonon, the associated relaxation time does depend on whether $\langle b \rangle_{t=0}$ is zero or not. To see this we note that $|\psi_{\rm ph}(x,t)|^2$ has two sources of time dependence originating from $\gamma(t)$ and $I_3(t)$. While $\gamma(t)$ decays to its asymptotic value γ with a relaxation time equal to $\tau/2$, $I_3(t)$ decays to zero with a relaxation time that is twice as long. The relaxation of $|\psi_{\rm ph}(x,t)|^2$ depends then on whether the expectation value on the right-hand side of Eq. (68) has a contribution that is linear in $I_3(t)$ and $I_3^*(t)$ or not. If $\langle b \rangle_{t=0} = 0$ there is no such linear contribution, hence $|\psi_{\rm ph}(x,t)|^2$ approaches its asymptotic form with the relaxation time $\tau/2$. If, on the other hand, $\langle b \rangle_{t=0}$ is nonzero then there is such a contribution and $|\psi_{\rm ph}(x,t)|^2$ relaxes on a longer time scale equal to τ.

Although Eq. (68) applies to any initial phonon state, of particular interest are those cases where the phonon initially occupies either a coherent state or an eigenstate of $\hat{n}_b = b^\dagger b$. If the initial state is a coherent state, i.e., $b|\psi_0\rangle = \lambda|\psi_0\rangle$, then

$$\langle e^{isI_3(t)b^\dagger} e^{isI_3^*(t)b} \rangle_{\rm b} = e^{is2{\rm Re}\{I_3^*(t)\lambda\}} = e^{isQ(t)}, \tag{73}$$

resulting in

$$|\psi_{\rm ph}(x,t)|^2 = \frac{1}{2\sqrt{\pi\gamma(t)}} \exp\left[-\frac{(x-Q(t))^2}{4\gamma(t)}\right]. \tag{74}$$

The phononic wave function is therefore a simple Gaussian, characterized by the time-dependent average $Q(t)$ and the time-dependent width $\sigma(t) = \sqrt{2\gamma(t)}$. If the initial state is an eigenstate of $\hat{n}_b$ with the eigenvalue n the phononic wave function is somewhat more convoluted, given by the formal expression

$$|\psi_{\rm ph}(x,t)|^2 = \sum_{m=0}^{n} \binom{n}{m} \frac{|I_3(t)|^{2m}}{2m!\sqrt{\pi\gamma(t)}} \frac{d^{2m}}{dx^{2m}} e^{-x^2/4\gamma(t)}. \tag{75}$$

Alternatively, Eq. (75) can be rewritten using Hermite polynomials as

$$|\psi_{\rm ph}(x,t)|^2 = \sum_{m=0}^{n} \binom{n}{m} \frac{|I_3(t)|^{2m}}{m!\sqrt{\pi}[4\gamma(t)]^{m+1/2}} H_n(y) e^{-y^2}, \tag{76}$$

with $y = x/\sqrt{4\gamma(t)}$.

The time evolution of the phononic wave function is displayed in Figs. 4 and 5 for two representative initial configurations of the phonon: a coherent state with $\lambda = 1$ (Fig. 4) and an eigenstate of $\hat{n}_b$ with the eigenvalue $n = 1$ (Fig. 5). Starting from a coherent state, the phononic wave function evolves through a sequence of Gaussians, as can be seen in Fig. 4. The center of the Gaussian, $Q(t)$, oscillates from $\sqrt{2}$ at time $t = 0$ to zero as $t \to \infty$ according to the black curve in Fig. 3, while its width increases form $1/\sqrt{2}$ to 1. In contrast, the phononic wave

function undergoes a qualitative change in shape when starting from $\hat{n}_d = 1$. Here $|\psi(x,t)|^2$ is initially composed of two symmetric peaks that gradually merge to a single Gaussian at long times. This behavior can be understood from the explicit form of Eq. (76) with $n = 1$:

$$|\psi_{\rm ph}(x,t)|^2 = \left[1 - \frac{|I_3(t)|^2}{2\gamma(t)} + \frac{|I_3(t)|^2}{4\gamma(t)^2}x^2\right] \frac{e^{-x^2/4\gamma(t)}}{2\sqrt{\pi\gamma(t)}}. \tag{77}$$

At $t = 0$ one can show that $|I_3(0)|^2 = 2\gamma(0) = 1/2$, resulting in

$$|\psi_{\rm ph}(x,t=0)|^2 = \frac{2}{\sqrt{\pi}}x^2 e^{-x^2}. \tag{78}$$

As time increases $|I_3(t)|^2$ gradually decays to zero, leaving us with the thermalized Gaussian of Eq. (72). The transition between the two forms of the wave function is therefore driven by the relaxation of $|I_3(t)|^2$, which happens on a time scale of $\tau/2$.

D. Thermalization in the presence of integrability

Tracking the time evolution of the phononic occupancy, displacement, and wave function in response to switching g on, we observed in the previous subsections that all quantities eventually approach their thermal equilibrium values with respect to the full Hamiltonian. In other words, the system thermalizes at long times. Indeed, this limit was rigorously shown by Ambegaokar[40] for a class of bosonic models that include our Hamiltonian of interest. More generally, it was shown by Doyon and Andrei[42] in the context of interacting quantum dots that

$$\lim_{t\to\infty} U^\dagger(t,0)e^{-\beta\mathcal{H}_0}U(t,0) = e^{-\beta\mathcal{H}}, \tag{79}$$

provided the bath is a large Fermi sea and $\mathcal{H} - \mathcal{H}_0$ is a local perturbation, as is the case here. However, one may wonder at this point how can an integrable system thermalize given the infinite set of conservation laws it possesses [specifically, the occupation numbers $\alpha_k^\dagger\alpha_k$, see Eq. (29)]?

To address this question consider the quench dynamics starting from an excited Fermi sea

$$|n_{k_1},\ldots,n_{k_N}\rangle_{g=0} = \left(a_{k_1}^\dagger\right)^{n_{k_1}}\cdots\left(a_{k_N}^\dagger\right)^{n_{k_N}}|0\rangle_{g=0}, \tag{80}$$

obtained by creating several particle-hole excitations with momenta $k_1, k_2, \ldots, k_N$ above the filled Fermi sea of the unperturbed system. Starting from the product state $|\psi_0\rangle = |n_b\rangle \otimes |n_{k_1},\ldots,n_{k_N}\rangle_{g=0}$ of the excited Fermi sea and a local phonon state with the occupation number n_b, one can repeat the calculation of Sec. IV B to track the time evolution of the phonon occupancy. At long time one finds

$$\begin{aligned} n_b(t\to\infty) &= \lambda^2\sum_{q>0}\xi_q^2\left|g(\epsilon_q+i\eta)\right|^2(\epsilon_q-\omega_0)^2 \\ &+ 2\lambda^2\sum_{j=1}^N\xi_{k_j}^2\left|g(\epsilon_{k_j}+i\eta)\right|^2\left(\epsilon_{k_j}^2+\omega_0^2\right)n_{k_j} \\ &= {}_g\langle n_{k_1},\ldots,n_{k_N}\left|b^\dagger b\right|n_{k_1},\ldots,n_{k_N}\rangle_g\,, \end{aligned} \tag{81}$$

where

$$|n_{k_1},\ldots,n_{k_N}\rangle_g = \left(\alpha_{k_1}^\dagger\right)^{n_{k_1}}\cdots\left(\alpha_{k_N}^\dagger\right)^{n_{k_N}}|0\rangle_g \tag{82}$$

is the corresponding eigenstate of the full Hamiltonian, obtained by creating scattering-state excitations with identical quantum numbers above the ground state of the full system. Thus, while the initial state of the local phonon is wiped out in the course of the evolution, the quantum numbers characterizing the initial state of the Fermi sea are preserved. In other terms, the conservation laws constrain the bulk but not the local degrees of freedom. Since $\xi_{k_j}^2$ scales as $1/L$, local observables are independent of the initial state of the Fermi sea as long as the initial excitation energy is not extensive, i.e.,

$$\frac{1}{L}\sum_{j=1}^N n_{k_j} \to 0 \tag{83}$$

in the thermodynamic limit. We therefore conclude that the local phonon thermalizes while the bath does not, and that the conservation laws which constrain the bath dynamics do allow for a generic evolution of local degrees of freedom.

V. ABRUPT CHANGE OF PHONON FREQUENCY

The second quench dynamics we consider is the response to a sudden change in the phonon frequency. Namely, the system is taken to occupy the ground state of the Hamiltonian of Eq. (23) at time $t = 0$ when the phonon frequency is abruptly shifted from ω_0 to $\omega_1 = \omega_0 + \delta\omega > 0$. In contrast to the electron-phonon coupling, which is difficult to control in actual devices, the frequency of vibrations can be tuned electrically in suspended carbon nanotubes.[43] This offers a potential realization of the present scenario. For concreteness we restrict attention in this section to $\epsilon_d = 0$ and zero temperature, though both restrictions can be relaxed. Accordingly, our interest will center on $n_b(t)$, as $Q(t)$ is pinned by symmetry to zero. Similarly, the phononic wave function retains a Gaussian form centered about $x = 0$ at arbitrary time t, with a time-dependent width equal to $\sqrt{\langle\hat{Q}^2(t)\rangle}$.

A. Time evolution of phononic operators

The general strategy for calculating the time evolution of physical observables is similar to the one taken in the

previous section, except that the initial Hamiltonian is now the full Hamiltonian $\mathcal{H}$ of Eq. (23) with $\tilde{\epsilon}_d$ set to zero, and the final Hamiltonian is given by $\mathcal{H}' = \mathcal{H} + \delta\mathcal{H}$ with

$$\delta\mathcal{H} = \delta\omega b^\dagger b. \tag{84}$$

The technical details are slightly more cumbersome, though, since the time evolution of $b^\dagger(t)$ is carried out by expanding $b^\dagger$ in terms of the eigenmodes γ_k and $\gamma_k^\dagger$ of the final Hamiltonian $\mathcal{H}'$, whereas the evaluation of expectation values requires an expansion of $b^\dagger(t)$ in terms of the eigenmodes α_k and $\alpha_k^\dagger$ of the initial Hamiltonian $\mathcal{H}$. In other words, one needs to know how to convert from the eigenmodes of $\mathcal{H}'$ to those of $\mathcal{H}$.

There are two approaches one can take to achieve this goal. The first is to invert Eq. (26) and its Hermitian conjugate in order to express a_q, $a_q^\dagger$, b and $b^\dagger$ in terms of the eigenmodes of $\mathcal{H}$, and to plug the resulting expressions into the expansion of $\gamma_k^\dagger$ in terms of a_q, $a_q^\dagger$, b and $b^\dagger$. An alternative approach is to directly express $\gamma_k^\dagger$ in terms of α_q and $\alpha_q^\dagger$ by solving the modified Lippmann-Schwinger equation

$$[\gamma_k^\dagger, \mathcal{H}'] = -\epsilon_k\gamma_k^\dagger + i\eta(\alpha_k^\dagger - \gamma_k^\dagger). \tag{85}$$

To this end, it is necessary to first write $\mathcal{H}'$ in terms of the eigenmodes of $\mathcal{H}$, which follows directly from Eqs. (29) and (32). As we prove in Appendix A, the two methods of computation are equivalent, allowing us to use the latter approach which is more concise. Differing all details of the calculation to the Appendix we quote here only the end result:

$$\begin{aligned}\gamma_k^\dagger \;=\; & \alpha_k^\dagger + 2\delta\omega\lambda^2\xi_k\tilde{g}(\epsilon_k + i\eta) \\ & \times\sum_{q>0}\xi_q\left[g(\epsilon_q - i\eta)\frac{\epsilon_k\epsilon_q + \omega_0\omega_1}{\epsilon_k - \epsilon_q + i\eta}\alpha_q^\dagger\right. \\ & \left. - g(\epsilon_q + i\eta)\frac{\epsilon_k\epsilon_q - \omega_0\omega_1}{\epsilon_k + \epsilon_q + i\eta}\alpha_q\right],\end{aligned} \tag{86}$$

where

$$\tilde{g}(z) = \frac{1}{z^2 - \omega_1^2 - 2\omega_1\Sigma(z)} \tag{87}$$

is the same function of Eq. (27) with ω_0 replaced by ω_1.

Since $\mathcal{H}'$ has the same exact form as the Hamiltonian $\mathcal{H}$ of Eq. (23) only with ω_0 replaced by ω_1, one can borrow all results derived previously in Sec. III for the latter Hamiltonian. In particular, $\mathcal{H}'$ is diagonal in the new basis set,

$$\mathcal{H}' = \sum_{k>0}\epsilon_k\gamma_k^\dagger\gamma_k, \tag{88}$$

and the expansions of $b^\dagger$ and $b^\dagger(t)$ detailed in Eqs. (32) and (33) still hold upon substituting ω_1, $\tilde{g}$, γ_k, and $\gamma_k^\dagger$ in for ω_0, g, α_k, and $\alpha_k^\dagger$, respectively. Plugging Eq. (86) and its Hermitian conjugate into Eq. (33) we finally obtain the desired expansion of $b^\dagger(t)$ in terms of the α_k's:

$$\begin{aligned} b^\dagger(t) \;=\; & \lambda\sum_{k>0}\xi_k\left[\tilde{g}(\epsilon_k - i\eta)(\epsilon_k + \omega_1)e^{i\epsilon_k t}\right. \\ & \left. + 2\delta\omega g(\epsilon_k - i\eta)J(\epsilon_k - i\eta, t)\right]\alpha_k^\dagger \\ & + \lambda\sum_{k>0}\xi_k\left[\tilde{g}(\epsilon_k + i\eta)(-\epsilon_k + \omega_1)e^{-i\epsilon_k t}\right. \\ & \left. + 2\delta\omega g(\epsilon_k + i\eta)J(-\epsilon_k - i\eta, t)\right]\alpha_k, \end{aligned} \tag{89}$$

where we have defined the auxiliary function

$$\begin{aligned} J(z,t) \;=\; & \lambda^2\sum_{k>0}\xi_k^2|\tilde{g}(\epsilon_k + i\eta)|^2\left[(\epsilon_k + \omega_1)\frac{\epsilon_k z + \omega_0\omega_1}{\epsilon_k - z}e^{i\epsilon_k t}\right. \\ & \left. + (\epsilon_k - \omega_1)\frac{\epsilon_k z - \omega_0\omega_1}{\epsilon_k + z}e^{-i\epsilon_k t}\right]. \end{aligned} \tag{90}$$

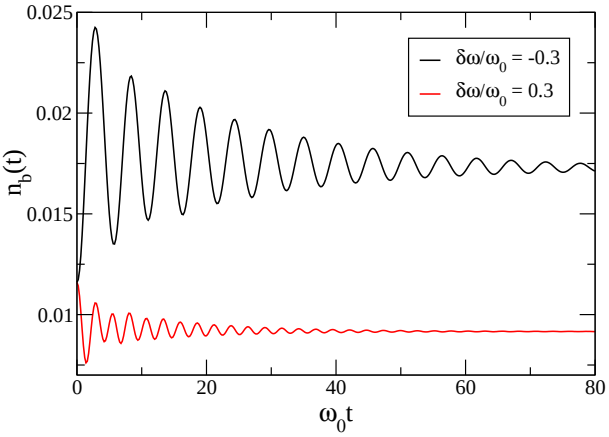

FIG. 6: (Color online) Time evolution of the phononic occupancy following an abrupt shift in the phonon frequency from $\omega_0/D_d = 0.2$ to $\omega_1 = \omega_0 + \delta\omega$ with $\delta\omega = \pm 0.3\omega_0$. The electron-phonon interaction is held fixed at $g/\Gamma = 0.324$.

B. Phononic occupancy

With Eq. (89) at hand, we are now in position to evaluate expectation values pertaining to the local phonon mode $b^\dagger$. Focusing on the time evolution of the phonon occupancy $n_b(t) = \langle b^\dagger(t)b(t)\rangle$, we note that $b^\dagger(t)b(t)$ is quadratic in $\alpha_k^\dagger$ and α_k. Since the expectation value is taken with respect to the ground state of the initial Hamiltonian $\mathcal{H}$, the only nonzero contributions stem from the diagonal terms $\alpha_k\alpha_k^\dagger$, resulting in

$$\begin{aligned} n_b(t) \;=\; & \lambda^2\sum_{k>0}\xi_k^2|\tilde{g}(\epsilon_k + i\eta)(-\epsilon_k + \omega_1)e^{-i\epsilon_k t} \\ & + 2\delta\omega g(\epsilon_k + i\eta)J(-\epsilon_k - i\eta, t)|^2. \end{aligned} \tag{91}$$

At $t = 0$, Eq. (91) properly reduces to the equilibrium expectation value of $\hat{n}_b$ with respect to $\mathcal{H}$ specified in Eq. (57). To see this we note that Eq. (89) must coincide

at time $t = 0$ with Eq. (32), as both expressions offer an expansion of $b^\dagger$ in terms of the α_k's and $\alpha_k^\dagger$'s. Equating the corresponding expansion coefficients one finds the identity

$$\begin{aligned} g(\epsilon_k + i\eta)(-\epsilon_k + \omega_0) &= 2\delta\omega g(\epsilon_k + i\eta)J(-\epsilon_k - i\eta, 0) \\ &+ \tilde{g}(\epsilon_k + i\eta)(-\epsilon_k + \omega_1), \end{aligned} \quad (92)$$

from which the equivalence of Eq. (57) and Eq. (91) at time $t = 0$ immediately follows. In the opposite limit of long times Eq. (91) reproduces the new equilibrium expectation value of $\hat{n}_b$ with respect to $\mathcal{H}'$. Indeed, using a similar analysis as beforehand one can show that $J(-\epsilon_k - i\eta, t)$ decays to zero with the same relaxation time τ and frequency of oscillations ω as listed in Eqs. (54) and (55), subject to the substitution of ω_0 with ω_1. This in turn leaves us at long times with

$$n_b(t \to \infty) = \lambda^2 \sum_{k>0} \xi_k^2 \left|\tilde{g}(\epsilon_k + i\eta)\right|^2 (\epsilon_k - \omega_1)^2, \quad (93)$$

which is the thermalized expectation value of $\hat{n}_b$ with respect to $\mathcal{H}'$. Thus, as expected, $n_b(t)$ interpolates between the two equilibria expectation values of $\hat{n}_b$.

Figure 6 shows the complete time evolution of $n_b(t)$ for two opposite shifts of the phonon frequency. Once again the curves take the form of damped oscillations with the relaxation time $\tau/2$ and the frequency of oscillations 2ω. Consequently, the decay time and frequency of oscillations differ substantially between $\delta\omega = 0.3\omega_0$ and $\delta\omega = -0.3\omega_0$, in accordance with the substitution $\omega_0 \to \omega_1 = (1 \pm 0.3)\omega_0$ in Eqs. (54) and (55). The larger is ω_1 the smaller are the new thermalized expectation value of $\hat{n}_b$ and the amplitude of damped oscillations that $n_b(t)$ undergoes.

VI. ABRUPT SHIFT OF ENERGY LEVEL

The third and final quench scenario we consider is the response to an abrupt shift in the electronic energy level, which has been held fixed up until now at resonance with the Fermi energy. Specifically, we assume that the system resides at time $t < 0$ in its ground state for $\epsilon_d = 0$, when a nonzero ϵ_d is suddenly switched on. This has the effect of breaking particle-hole symmetry, dynamically generating a nonzero displacement $Q(t)$ of the local phonon along with deviations of the level occupancy from half filling [i.e., $n_d(t) \neq 1/2$]. These two observables will be our main focus of interest. Of the different quench scenarios under consideration the present one is by far the most accessible experimentally, as the energy level ϵ_d can be controlled quite efficiently using suitable gate voltages.

The foundations for calculating $Q(t)$ and $n_d(t)$ in this scenario have been laid down in Sec. III B. Specifically, from Eq. (38) one has that

$$\begin{aligned} \tilde{b}^\dagger(t) &= \lambda \sum_{k>0} \xi_k \Big[g(\epsilon_k - i\eta)(\epsilon_k + \omega_0) e^{i\epsilon_k t} \beta_k^\dagger \\ &\quad - g(\epsilon_k + i\eta)(\epsilon_k - \omega_0) e^{-i\epsilon_k t} \beta_k \Big] \end{aligned} \quad (94)$$

which, when combined with Eqs. (36) and (39), yields

$$\begin{aligned} b^\dagger(t) &= h_1(t) + \lambda \sum_{k>0} \xi_k \Big[g(\epsilon_k - i\eta)(\epsilon_k + \omega_0) e^{i\epsilon_k t} \alpha_k^\dagger \\ &\quad - g(\epsilon_k + i\eta)(\epsilon_k - \omega_0) e^{-i\epsilon_k t} \alpha_k \Big] \end{aligned} \quad (95)$$

with

$$\begin{aligned} h_1(t) &= \lambda \tilde{\epsilon}_d \sum_{k>0} \xi_k^2 |g(\epsilon_k + i\eta)|^2 (\epsilon_k^2 - \omega_0^2) \\ &\quad \times \left[\frac{\epsilon_k + \omega_0}{\epsilon_k + i\eta} e^{i\epsilon_k t} - \frac{\epsilon_k - \omega_0}{\epsilon_k - i\eta} e^{-i\epsilon_k t} \right] \\ &+ \frac{\epsilon_d}{\pi\Gamma} \frac{g}{\omega_0} \frac{1}{1 - 2g^2/(\pi\omega_0\Gamma)}. \end{aligned} \quad (96)$$

Accordingly, the phonon displacement is equal to $Q(t) = \sqrt{2}\mathrm{Re}\{h_1(t)\}$, which follows from the fact that α_k and $\alpha_k^\dagger$ average to zero with respect to the initial state. Similarly from Eq. (41) one has that

$$\tilde{n}_d(t) = \frac{1}{2} + a \sum_{k>0} \xi_k (\epsilon_k^2 - \omega_0^2) \left[g(\epsilon_k - i\eta) e^{i\epsilon_k t} \beta_k^\dagger + \mathrm{H.c.} \right] \quad (97)$$

which, when combined with Eqs. (36) and (42), yields

$$\tilde{n}_d(t) = h_2(t) + a \sum_{k>0} \xi_k (\epsilon_k^2 - \omega_0^2) \left[g(\epsilon_k - i\eta) e^{i\epsilon_k t} \alpha_k^\dagger + \mathrm{H.c.} \right] \quad (98)$$

with

$$\begin{aligned} h_2(t) &= \frac{1}{2} - \frac{\epsilon_d}{\pi\Gamma} \frac{1}{1 - 2g^2/(\pi\omega_0\Gamma)} \\ &+ \tilde{\epsilon}_d a \sum_{k>0} \xi_k^2 |g(\epsilon_k + i\eta)|^2 (\epsilon_k^2 - \omega_0^2)^2 \\ &\quad \times \left[\frac{e^{i\epsilon_k t}}{\epsilon_k + i\eta} + \frac{e^{-i\epsilon_k t}}{\epsilon_k - i\eta} \right]. \end{aligned} \quad (99)$$

Hence the occupancy of the localized level is simply given by $n_d(t) = h_2(t)$.

The occupancy $n_d(t)$ of the localized electronic level is depicted in Fig. 7. Several points are noteworthy. First, $n_d(t) - 1/2$ depends linearly on ϵ_d in our solution. This property stems from the fact that ϵ_d couples linearly to the bosonic degrees of freedom, in accord with the assumption that $|\epsilon_d| \ll \Gamma$. Indeed, as $|\epsilon_d|$ is increased the mapping onto the bosonic Hamiltonian of Eq. (23) gradually breaks down, generating higher order corrections in ϵ_d.

Second, the dynamics of $n_d(t)$ is composed of two distinct segments: fast dynamics on the scale of $1/D_d \sim 1/\Gamma$, where most of the charge redistribution takes place, followed by an extended region of damped oscillations.

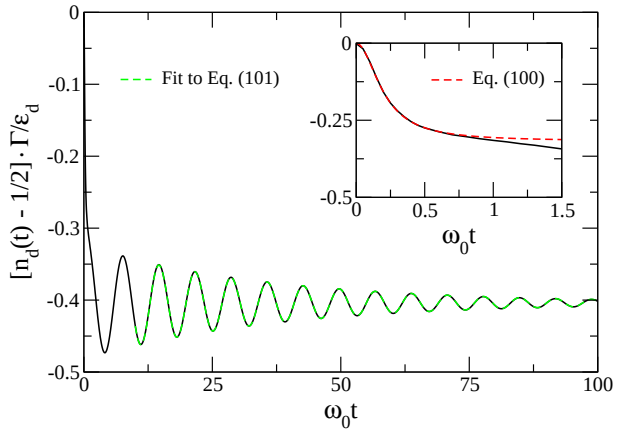

FIG. 7: (Color online) Time evolution of the occupancy $n_d(t)$ of the localized electronic level, following an abrupt change in its energy from $\epsilon_d = 0$ to $\epsilon_d \neq 0$. Here $\omega_0/D_d = 0.2$ and $g/\Gamma = 0.324$. Note that $n_d(t) - 1/2$ depends linearly on ϵ_d. The green dashed line shows a fit to Eq. (101) using the fitting range $10 \leq \omega_0 t \leq 100$. Inset: A zoom in on the short-time behavior. The red dashed curve shows the analytical form of Eq. (100).

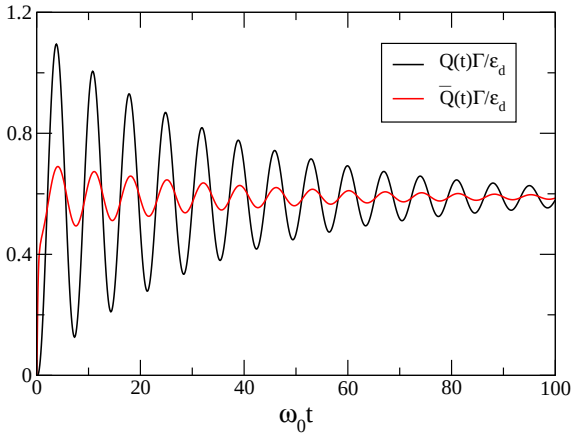

FIG. 8: (Color online) Time evolution of the displacement $Q(t)$, following an abrupt change in the level energy from $\epsilon_d = 0$ to $\epsilon_d \neq 0$. All model parameters are the same as in Fig. 7. For comparison, the red curve plots $\bar{Q}(t)$ of Eq. (106).

The short-time dynamics originates from the high-energy end of the summation over k in Eq. (99), and is given by

$$n_d(t) = \frac{1}{2} - \frac{\epsilon_d}{\pi\Gamma}\frac{(tD_d)^2}{1+(tD_d)^2} \tag{100}$$

(see inset of Fig. 7). This simple analytical form stems from the exponential high-energy cutoff imposed by ξ_k^2 [see Eq. (22)]. While the functional form of $n_d(t)$ may differ from Eq. (100) for other cutoff schemes, the relevant time scale $t \sim 1/\Gamma$ and the characteristic change in occupancy $\delta n_d \sim \epsilon_d/\pi\Gamma$ experienced within this time segment should be generic. As for the damped oscillations, these are expected to take the functional form

$$n_d(t) = A\sin(\Omega t + \phi)e^{-t/\tau_0} + C \tag{101}$$

with Ω and τ_0 equal to ω and τ. We confirm this form in Fig. 7, where the fitted values of Ω and τ_0 agree to within 0.1% with those extracted from Fig. 1 by fitting $n_b(t)$ to Eq. (58).[41]

Lastly, from the asymptotic long-time behavior of $n_b(t)$ one can deduce the dimensionless parameter controlling the perturbative expansion in g in thermal equilibrium. For $g = 0$ and arbitrary ϵ_d, the exact equilibrium occupancy of the electronic level is given by the standard expression

$$n_d = \frac{1}{2} - \frac{1}{\pi}\arctan\left(\frac{\epsilon_d}{\Gamma}\right), \tag{102}$$

which reduces to $n_d = 1/2 - \epsilon_d/\pi\Gamma$ for $|\epsilon_d| \ll \Gamma$. This latter result is accurately reproduced by our treatment upon setting g equal to zero. For nonzero g we find that

$$n_d = \frac{1}{2} - \frac{\epsilon_d}{\pi\Gamma}\frac{1}{1-2g^2/(\pi\omega_0\Gamma)}, \tag{103}$$

revealing that the true expansion parameter is $g^2/\omega_0\Gamma$, i.e., the ratio of the polaronic shift g^2/ω_0 to the hybridization width Γ. The effect of the electron-phonon coupling g is to increase the deviation from half filling for a given value of ϵ_d, signaling a narrowing of the electronic resonance according to

$$\Gamma \to \Gamma_{\rm eff} = \Gamma - \frac{2g^2}{\pi\omega_0}. \tag{104}$$

The time evolution of the phonon displacement is plotted in turn in Fig. 8. Similar to the level occupancy, $Q(t)$ depends linearly on ϵ_d and undergoes damped oscillations with the relaxation time τ and frequency ω. It lacks, however, the fast dynamics that the level occupancy experiences on the time scale of $1/\Gamma$. In equilibrium n_d and Q are related through

$$Q = -\sqrt{2}\frac{g}{\omega_0}\left[n_d - \frac{1}{2}\right], \tag{105}$$

which is an exact result applicable to arbitrary ϵ_d, ω_0, and g.[44] It is thus natural to ask whether this general relation extends to nonequilibrium dynamics. To this end, in Fig. 8 we have plotted

$$\bar{Q}(t) = -\sqrt{2}\frac{g}{\omega_0}\left[n_d(t) - \frac{1}{2}\right] \tag{106}$$

alongside $Q(t)$. Although nearly in phase, the two quantities are characterized by vastly different amplitudes of oscillations, marking the breakdown of Eq. (105) under nonequilibrium dynamics. The latter relation is restored only asymptotically as the system thermalizes.

VII. DRIVEN DYNAMICS

Up until now we considered the response to a single quantum quench. Quantum control of nanodevices often

requires the usage of driven dynamics, where periodic forcing is applied to the system. Such drives are a theoretical challenge to describe since the system not only remains permanently remote from thermal equilibrium, but it never even reaches steady state. Remarkably, we are able to extend our exact solution to a rather broad class of driven dynamics where the forcing couples linearly to the bosonic degrees of freedom. As we discuss below, this class of drives includes at least two physically relevant scenarios where periodic forcing is applied either to the localized phonon or to the electronic level. Accordingly, we begin our derivation with a general discussion of this class of drives before turning to the two concrete examples of interest.

A. Drives that couple linearly to bosons

The general setting we consider consists of a system that resides at time $t<0$ in thermal equilibrium, when a time-dependent drive is suddenly applied to it. In formal terms, the Hamiltonian of the system is changed abruptly at time $t=0$ from the Hamiltonian $\mathcal{H}$ of Eq. (23) to $\mathcal{H}'(t)=\mathcal{H}+\mathcal{H}_{\rm drive}(t)$ with

$$\mathcal{H}_{\rm drive}(t)=\sum_{k>0}\Big[M_k(t)\alpha_k^\dagger+M_k^*(t)\alpha_k\Big]. \tag{107}$$

Here we have assumed that the drive couples linearly to the eigenmodes of $\mathcal{H}$, exploiting the fact that any linear combination of the original bosonic degrees of freedom can be expanded in terms of the scattering-state operators α_k and $\alpha_k^\dagger$. The coefficients $M_k(t)$ depend on the exact scenario under consideration and will typically have the separable form $M_k(t)=A(t)m_k$. Nevertheless, we shall regard them for the time being as general coefficients without making any further assumption about their form. The initial value of the energy level ϵ_d will be taken for simplicity to be zero, though the extension to nonzero ϵ_d is quite straightforward.

A convenient way to incorporate the time-dependent drive is via the Heisenberg equation of motion for the scattering-state operators, which takes the form

$$\dot\alpha_k(t)=-i\epsilon_k\alpha_k(t)-iM_k(t), \tag{108}$$

subject to the initial condition $\alpha_k(t=0)=\alpha_k$. Here the first term on the right-hand side of Eq. (108) is due to $\mathcal{H}$ and the second term is due to $\mathcal{H}_{\rm drive}$. Equation (108) has the formal solution

$$\alpha_k(t)=\alpha_k e^{-i\epsilon_k t}-i\int_0^t e^{i\epsilon_k(t'-t)}M_k(t')dt', \tag{109}$$

from which the time evolution of all physical operators of interest can be deduced. For example, combining Eq. (32) with Eq. (109) and its Hermitian conjugate one obtains

$$b^\dagger(t)=b_0^\dagger(t)+i\lambda\mathcal{B}(t), \tag{110}$$

where $b_0^\dagger(t)$ is the time-evolved operator in the absence of a drive [see Eq. (33)] and $\mathcal{B}(t)$ is a time-dependent shift given by

$$\mathcal{B}(t)=\sum_{k>0}\xi_k\Big[g(\epsilon_k-i\eta)(\epsilon_k+\omega_0)\int_0^t M_k^*(t')e^{-i\epsilon_k(t'-t)}dt' +g(\epsilon_k+i\eta)(\epsilon_k-\omega_0)\int_0^t M_k(t')e^{i\epsilon_k(t'-t)}dt'\Big]. \tag{111}$$

Accordingly, the phonon displacement takes the form

$$Q(t)=-\sqrt{2}\lambda{\rm Im}\{\mathcal{B}(t)\}, \tag{112}$$

while its occupancy reads

$$n_b(t)=n_b^{(0)}+\lambda^2|\mathcal{B}(t)|^2. \tag{113}$$

Here $n_b^{(0)}$ denotes the equilibrium phononic occupancy in the absence of a drive, given by Eq. (57) for $T=0$. Note that in deriving Eqs. (112) and (113) we have made use of the fact that $b(t)+b^\dagger(t)$ and $b^\dagger(t)b(t)$ are averaged with respect to the equilibrium density operator corresponding to $\mathcal{H}$, which is diagonal in the occupation numbers $\alpha_k^\dagger\alpha_k$. As a result $\langle\alpha_k\rangle$ and $\langle\alpha_k^\dagger\rangle$ identically vanish. A similar calculation for the time-dependent occupancy $\delta n_d(t)=n_d(t)-1/2$ of the localized level yields

$$\delta n_d=a\sum_{k>0}\xi_k(\epsilon_k^2-\omega_0^2)\big[-ig(\epsilon_k+i\eta)\int_0^t M_k(t')e^{i\epsilon_k(t'-t)}dt' +ig(\epsilon_k-i\eta)\int_0^t M_k^*(t')e^{-i\epsilon_k(t'-t)}dt'\big]. \tag{114}$$

Equations (113) and (114) combined provide us with a formal solution for the occupancies of the local phonon and the electronic level for a general drive. Furthermore, these expressions apply to arbitrary temperature T, provided $n_b^{(0)}$ is taken to be the equilibrium phononic occupancy at that temperature. Below we utilize these expressions to analyze two cases of practical interest, where ac forcing is applied either to the local phonon or to the localized level.

B. ac forcing of the local phonon

In the first scenario to be analyzed, ac forcing is applied at time $t>0$ to the local phonon, as described by the Hamiltonian term

$$\mathcal{H}_{\rm drive}(t)=\Delta\sin(\Omega t)(b^\dagger+b). \tag{115}$$

Here Δ, which has dimensions of energy, is the amplitude of the drive and Ω is the driving frequency (not to be confused with the fitting parameter previously used for analyzing the damped oscillations). Such forcing can be applied, e.g., to polar molecules using an ac electric field.

Using the expansion of $b^\dagger$ in terms of the scattering-state operators given in Eq. (32), the Hamiltonian term

of Eq. (115) can be recast in the form of Eq. (107) with the coefficients

$$M_k(t) = 2\omega_0\lambda\Delta\sin(\Omega t)\xi_k g(\epsilon_k - i\eta), \tag{116}$$

such that

$$\int_0^t M_k^*(t')e^{-i\epsilon_k(t'-t)}dt' = \omega_0\lambda\Delta\xi_k g(\epsilon_k + i\eta)\zeta_k(t) \tag{117}$$

with

$$\zeta_k(t) = \frac{e^{i\Omega t} - e^{i\epsilon_k t}}{\epsilon_k - \Omega} - \frac{e^{-i\Omega t} - e^{i\epsilon_k t}}{\epsilon_k + \Omega}. \tag{118}$$

For computational convenience it is useful to add an infinitesimal imaginary part $i\eta$ to the denominators in Eq. (118), thereby rewriting $\zeta_k(t)$ as[45]

$$\zeta_k(t) = \frac{e^{i\Omega t} - e^{i\epsilon_k t}}{\epsilon_k - \Omega + i\eta} - \frac{e^{-i\Omega t} - e^{i\epsilon_k t}}{\epsilon_k + \Omega + i\eta}. \tag{119}$$

A somewhat lengthy calculation then gives

$$\lambda\mathcal{B}(t) = \frac{\Delta}{2}\left[F(-\Omega - i\eta, t) - F(\Omega - i\eta, t)\right], \tag{120}$$

where $F(z,t)$ is the same function defined in Eq. (47). The phonon displacement and occupancy therefore take the rather compact forms

$$Q(t) = -\frac{\Delta}{\sqrt{2}}\mathrm{Im}\{F(-\Omega - i\eta, t) - F(\Omega - i\eta, t)\} \tag{121}$$

and

$$n_b(t) = n_b^{(0)} + \frac{\Delta^2}{4}|F(-\Omega - i\eta, t) - F(\Omega - i\eta, t)|^2. \tag{122}$$

The general structure of $Q(t)$ and $n_b(t)$ could be understood from properties of the function $F(z,t)$. Since $F(z,0)$ identically vanishes for arbitrary z, the phononic occupancy and displacement properly reduce at time $t = 0$ to their thermal equilibrium values, as they physically should. As soon as $t > 0$, the two components of $F(\pm\Omega - i\eta)$ behave markedly differently. The first term in Eq. (47) oscillates indefinitely with frequency Ω, whereas the term involving the sum over k undergoes damped oscillations with the relaxation time τ and frequency ω of Eqs. (55) and (54), respectively. Thus, there is a clear distinction between the roles of the two terms: while the first term in Eq. (47) survives at long times and is responsible for the long-time behavior, the second term contains all transients that decay in time. This leads to the following characterization of $Q(t)$ and $n_b(t)$. At short times, $t < \tau$, the phonon displacement comprises of two components oscillating at frequencies Ω and ω, while $n_b(t)$ contains four distinct oscillatory terms with the frequencies 2Ω, $\Omega \pm \omega$, and 2ω. At long times, $\tau \ll t$, the phonon displacement oscillates with frequency Ω about zero, while $n_b(t)$ oscillates with frequency 2Ω about a new time-averaged value $\bar{n}_b$. Explicitly, $Q(t)$ and $\delta n_b(t) = n_b(t) - n_b^{(0)}$ reduce at long times to

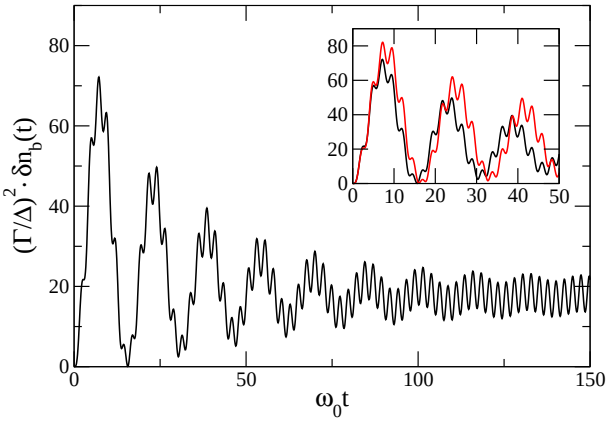

FIG. 9: (Color online) Time evolution of $\delta n_b(t) = n_b(t) - n_b^{(0)}$ in response to ac forcing of the phonon according to $\mathcal{H}_{\rm drive}(t)$ of Eq. (115). Here $\omega_0/D_d = 0.2$, $g/\Gamma = 0.28$, and $\Omega = 1.3\omega_0$. Initially there is a rich structure involving the interference of four distinct frequencies. As transients decay (on a time scale of τ), $\delta n_b(t)$ gradually reduces to a single harmonic with a frequency of oscillations equal to 2Ω. Inset: Zoom in on the earlier time segment $\omega_0 t < 50$, including a comparison to the stronger coupling strength $g/\Gamma = 0.324$ (red curve).

$$Q(t) = \sqrt{2}\Delta\omega_0|g(\Omega + i\eta)|\sin(\Omega t + \phi) \tag{123}$$

and

$$\delta n_b(t) = \frac{\Delta^2}{2}|g(\Omega + i\eta)|^2\left[\omega_0^2 + \Omega^2 + \left(\Omega^2 - \omega_0^2\right)\cos(2\Omega t + 2\phi)\right], \tag{124}$$

with $\phi = \arg\{g(\Omega - i\eta)\}$.

On physical grounds one expects the response to an ac drive to reduce at long times to a periodic function of time, containing all harmonics of the driving frequency Ω. Surprisingly, the oscillatory parts of $Q(t)$ and $\delta n_b(t)$ consist in this limit of just a single harmonic each. While $Q(t)$ tracks the driving field with a phase difference of ϕ, $\delta n_b(t)$ oscillates with the doubled frequency 2Ω, lacking any signal at the principal harmonic Ω. Such behavior is quite atypical, as is the absence of higher harmonics. We expect both features to qualitatively change as the electron-phonon coupling is increased beyond the validity of our solution. We further note that the doubling of frequency in $\delta n_b(t)$ is reminiscent of a similar doubling of frequency in the damped oscillations that $n_b(t)$ undergoes in response to a quantum quench (see, e.g., Figs. 1 and 3 and their accompanying texts).

Focusing on $\delta n_b(t)$, its amplitude depends in a simple quadratic manner on Δ. Other than setting the overall amplitude, Δ has no additional effect on $\delta n_b(t)$. By contrast, the shape of $\delta n_b(t)$ is quite sensitive to the driving frequency Ω, as demonstrated in Figs. 9 and 10. When Ω is tuned off-resonance with the intrinsic frequency ω of the system, see Fig. 9, the transient behavior shows a

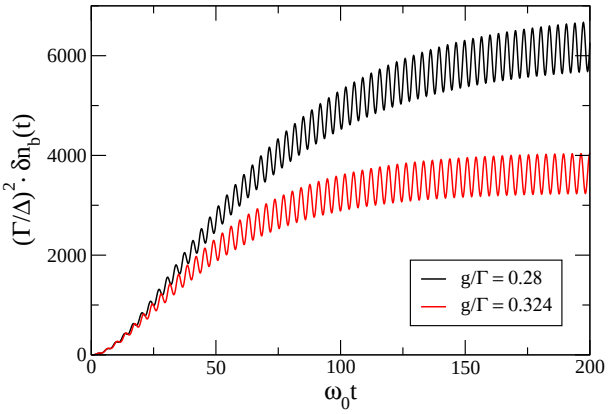

FIG. 10: (Color online) Same as Fig. 9, with Ω tuned to the resonance frequency: $\omega = 0.896\omega_0$ for $g/\Gamma = 0.324$ and $\omega = 0.923\omega_0$ for $g/\Gamma = 0.28$. All other model parameters are the same as in Fig. 9. Note the vastly different vertical scale as compared to that used in Fig. 9.

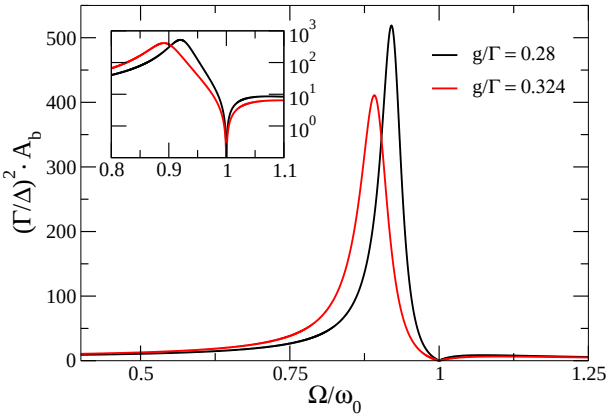

FIG. 11: (Color online) The asymptotic long-time amplitude of oscillations A_b vs the driving frequency Ω, for $\omega_0/D_d = 0.2$ and two different strengths of the electron-phonon coupling g. Inset: A zoom in on the vicinity of the resonance peak. A logarithmic scale is used for the y ordinate so as to emphasize the vanishing of A_b for $\Omega = \omega_0$.

rather rich structure that stems from the interference of the four underlying frequencies 2Ω, $\Omega \pm \omega$, and 2ω. Only after all transients have decayed on a time scale of τ does $\delta n_b(t)$ approach its asymptotic long-time form of a single harmonic with the doubled frequency 2Ω.

A rather different picture is recovered when Ω is tuned to the resonance frequency ω, see Fig. 10. Here both the transient and long-time behaviors are governed by the same single frequency $2\Omega = 2\omega$, resulting in much smoother curves. Quite striking is the substantial increase of the amplitude of oscillations upon approaching the resonance frequency. Indeed, the amplitude of the long-time oscillations is roughly two orders of magnitude larger in Fig. 10 as compared to Fig. 9, which is readily understood from Eq. (124). Since the amplitude of oscillations is given at long times by

$$A_b = \frac{\Delta^2}{2}|g(\Omega + i\eta)|^2|\omega_0^2 - \Omega^2|, \tag{125}$$

it displays a sharp resonance for $\Omega \approx \omega$ where $|g(\Omega + i\eta)|$ is sharply peaked.[46] The amplitude of oscillations at resonance can be crudely estimated as

$$A_b^{\rm res} \sim \frac{(\Delta\tau)^2}{8\omega^2}|\omega_0^2 - \omega^2|, \tag{126}$$

with ω and τ approximately given by Eqs. (54) and (55), respectively. Another interesting observation is the vanishing of A_b for $\Omega = \omega_0$. A plot of the amplitude A_b of the long-time oscillations as a function of Ω is depicted in Fig. 11.

C. ac forcing of local electronic level

In the second scenario that we analyze, ac forcing is applied at time $t > 0$ to the localized electronic level, as described by the Hamiltonian term

$$\mathcal{H}_{\rm drive}(t) = \Delta \sin(\Omega t)\left(\hat{n}_d - \frac{1}{2}\right). \tag{127}$$

Here, as before, Δ denotes the amplitude of the drive and Ω is the forcing frequency. Experimentally such a drive can be realized by applying microwave voltage to a nearby plunger gate, similar to the setups used by Elzerman *et al.*[47] and by Kogan *et al.*[48] in their respective studies of the ac Kondo effect in semiconductor quantum dots.

Using the mode expansion of Eq. (34) one can again recast the Hamiltonian term of Eq. (127) in the form of Eq. (107), this time with the coefficients

$$M_k(t) = \Delta a \sin(\Omega t)\xi_k g(\epsilon_k - i\eta)(\epsilon_k^2 - \omega_0^2). \tag{128}$$

Repeating the same sequence of steps detailed in Eqs. (117)–(119) and plugging the resulting expressions into Eq. (114), one obtains after a rather lengthy calculation

$$\delta n_d(t) \equiv n_d(t) - \frac{1}{2} = \frac{\Delta}{g^2}{\rm Im}\{\tilde{F}(\Omega - i\eta, t)\} \tag{129}$$

with

$$\begin{aligned}\tilde{F}(z,t) \;=\; & (z^2 - \omega_0^2)g(z)\Sigma(z)e^{izt} + \lambda^2 \sum_{k>0}\xi_k^2|g(\epsilon_k + i\eta)|^2 \\ & \times \left(z^2 - \omega_0^2\right)^2\left(\frac{e^{i\epsilon_k t}}{\epsilon_k - z} + \frac{e^{-i\epsilon_k t}}{\epsilon_k + z}\right).\end{aligned} \tag{130}$$

The function $\tilde{F}(z,t)$ has similar properties to those of $F(z,t)$. At $t = 0$ it vanishes identically for any value of z, and is composed of two distinct components for $t > 0$: one that oscillates indefinitely with frequency Ω, and another that oscillates with frequency ω and decays with the relaxation time τ for any z in the lower

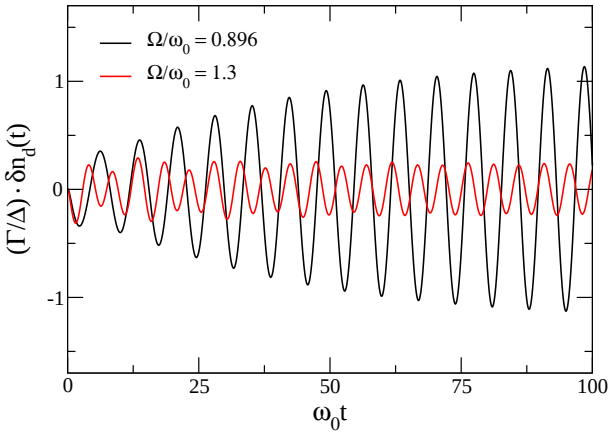

FIG. 12: (Color online) Time evolution of $\delta n_d(t)$ in response to ac forcing of the local electronic level according to $\mathcal{H}_{\rm drive}(t)$ of Eq. (127). Here $\omega_0/D_d = 0.2$ and $g/\Gamma = 0.324$. Two driving frequencies are shown, one ($\Omega = 1.3\omega_0$) off resonance and the other ($\Omega = 0.896\omega_0$) on resonance with the internal frequency ω.

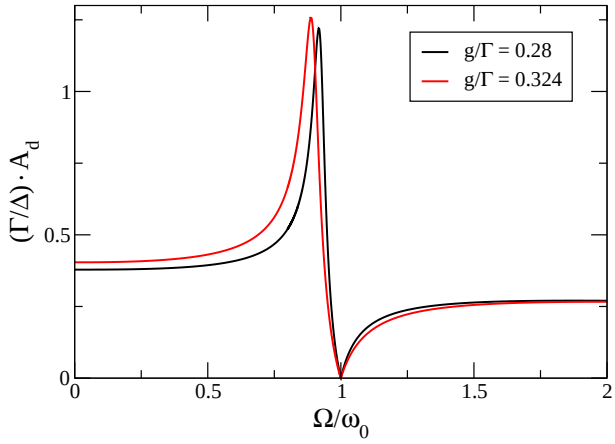

FIG. 13: (Color online) The asymptotic long-time amplitude of oscillations A_d vs the driving frequency Ω, for $\omega_0/D_d = 0.2$ and two different strengths of the electron-phonon coupling g.

half plane. Since $\delta n_d(t)$ is proportional to the imaginary part of $\tilde{F}(\Omega - i\eta, t)$ [as opposed to $\delta n_b(t)$ that depends quadratically on $F(\pm\Omega - i\eta, t)$] it comprises at short times $t < \tau$ of two oscillatory terms, one with frequency Ω and another with frequency ω. As t exceeds τ the latter component is progressively suppressed and $\delta n_d(t)$ gradually approaches its asymptotic long-time form

$$\delta n_d(t) = A_d \sin(\Omega t + \varphi), \tag{131}$$

with

$$A_d = \frac{\Delta}{g^2} |(\Omega^2 - \omega_0^2) g(\Omega + i\eta) \Sigma(\Omega + i\eta)| \tag{132}$$

and $\varphi = \arg\left\{(\Omega^2 - \omega_0^2) g(\Omega - i\eta)\Sigma(\Omega - i\eta)\right\}$. As beforehand, the long-time oscillations develop a resonance for $\Omega \approx \omega$, albeit with a reduced amplitude as compared to A_b of Eq. (125). This reduction in amplitude stems from a weaker linear dependence of A_d on $|g(\Omega + i\eta)|$. Similar to A_b, the amplitude of oscillations is suppressed to zero for $\Omega = \omega_0$, leaving no signal at long times for this particular frequency. A summary of our results is presented in Figs. 12 and 13.

VIII. SUMMARY AND CONCLUSIONS

In this paper we have presented an asymptotically exact solution for the nonequilibrium dynamics of a single-molecule transistor in response to various quantum quenches and drives. Our solution, which is based on a controlled mapping of the original Hamiltonian of Eq. (1) onto a form quadratic in bosonic operators,[24] is formally confined to weak electron-phonon coupling and near-resonance conditions for the electronic level: $\Gamma \gg \max\{g, |\epsilon_d|, g^2/\omega_0\}$. While some aspects of this regime can be accessed using ordinary perturbation theory in g, the ability to sum all orders exactly allowed us to (i) explicitly show how the system thermalizes following a quantum quench, (ii) identify the different time scales that govern the dynamics of the system, and (iii) access the asymptotic long-time response to a periodic drive.

Transient behaviors following a quantum quench were found to involve two characteristic scales[24] — an intrinsic frequency ω and a relaxation time τ approximately given by Eqs. (54) and (55), respectively. Quite surprisingly, some observables, such as the phonon displacement and the electronic occupancy of the localized level, display damped oscillations with frequency ω and the relaxation time τ, while other observables, such as the phononic occupancy, oscillate with frequency 2ω and decay with the reduced relaxation time $\tau/2$. The distinction has to do with the bosonic representation of the observable in question. If the latter is expressed as a linear combination of bosonic operators, the relevant frequency and decay time are ω and τ. If, on the other hand, the the observable in question is quadratic in bosonic operators, the relevant frequency and decay time are 2ω and $\tau/2$, respectively.

A special feature of our solution is the nature of the long-time response of observables to ac drives, whose oscillatory component reduces to just a single harmonic with an amplitude that depends in a simple power-law fashion on the forcing amplitude Δ. The absence of additional harmonics in the long-time ac response is a direct consequence of the mapping onto a free bosonic Hamiltonian with a forcing field that couples linearly to the bosonic modes. Physically this implies that other harmonics, which are generally expected to exist for the original Hamiltonian of Eq. (1), are parametrically small for $\Gamma \gg \max\{g, g^2/\omega_0\}$. As the electron-phonon interaction is increased such that $\max\{g, g^2/\omega_0\}$ approaches Γ, additional harmonics are expected to gain significance, that is provided the forcing amplitude Δ is not too small.

Concomitantly, the amplitudes of the different harmonics should gradually acquire a more elaborate dependence on Δ beyond a simple power-law form. We emphasize that this regime can no longer be described by the bosonic Hamiltonian of Eq. (23).

It would be interesting to compare our results with a numerical evaluation of the quench dynamics using, e.g., the time-dependent numerical renormalization group (TD-NRG).[9,10] Since ω and τ are independent of the high-energy cutoff used in the electronic Hamiltonian of Eqs. (1) and (2), this should facilitate a direct comparison between the two approaches on time scales exceeding $1/D_d \sim 1/\Gamma$. The precise forms of ω and τ, as well as the short-time dynamics up to $t \sim 1/\Gamma$, do depend on the cutoff scheme used for the bosonized Hamiltonian of Eq. (23). Nevertheless, we expect our weak-coupling expressions for ω and τ to apply in their present forms, as these coincide with low-order perturbation theory in g when applied directly to the electronic Hamiltonian of Eq. (1).

The true power of the TD-NRG lies, however, in its ability to treat arbitrary couplings strengths, which should enable one to go beyond the weak-coupling regime covered in this paper. It would be particularly interesting to see which aspects of our solution persist away from weak coupling, and what are the new qualitative features that are introduced as the electron-phonon coupling is increased. The study of stronger couplings along these lines is left for future work.

Acknowledgments

This work was supported in part by the US-Israel Binational Science Foundation through grant no. 2008440. YV is grateful to the condensed matter theory group at Rutgers university for their kind hospitality during the early stages of this work.

Appendix A: Solution of the scattering-state operators

In this Appendix, we detail the solution of the scattering-state operators for the different cases covered in the main text. Altogether three cases are considered: (i) a level at resonance with the Fermi energy, i.e., $\epsilon_d = 0$, (ii) a level off-resonance with the Fermi level, i.e., $\epsilon_d \neq 0$, and (iii) a local phonon with the shifted frequency $\omega_1 = \omega_0 + \delta\omega$. As emphasized in the main text, in the latter case we are interested in expanding the scattering-state operators corresponding to the frequency ω_1 in terms of those corresponding to the original frequency ω_0.

1. A level at resonance with the Fermi energy

We begin with a level at resonance with the Fermi energy, corresponding to the Hamiltonian of Eq. (23) with $\tilde{\epsilon}_d = 0$. Our objective is to solve the Lippmann-Schwinger equation

$$\left[\alpha_k^\dagger, \mathcal{H}\right] = -\epsilon_k \alpha_k^\dagger + i\eta\big(a_k^\dagger - \alpha_k^\dagger\big), \tag{A1}$$

where $\eta \to 0^+$ is a positive infinitesimal. To this end, we employ the methodology developed in Ref. 35. Introducing the Liouville operator $\mathcal{L}\hat{O} = \left[\hat{O}, \mathcal{H}\right]$, Eq. (A1) is rewritten in the form

$$\big(\mathcal{L} + \epsilon_k + i\eta\big)\alpha_k^\dagger = i\eta a_k^\dagger, \tag{A2}$$

which has the formal solution

$$\alpha_k^\dagger = \frac{i\eta}{\mathcal{L} + \epsilon_k + i\eta} a_k^\dagger. \tag{A3}$$

Next we divide the Hamiltonian $\mathcal{H}$ into three parts,

$$\mathcal{H}_0 = \sum_{k>0} \epsilon_k a_k^\dagger a_k, \tag{A4}$$

$$\mathcal{H}_1 = \omega_0 b^\dagger b, \tag{A5}$$

$$\mathcal{H}_2 = \lambda(b^\dagger + b) \sum_{q>0} \xi_q \left(a_q + a_q^\dagger\right), \tag{A6}$$

and associate each Hamiltonian term with its own Liouville operator: $\mathcal{L}_n\hat{O} = \left[\hat{O}, \mathcal{H}_n\right]$ $(n = 0, 1, 2)$. Using the operator identity

$$\frac{1}{\mathcal{L} + \epsilon_k + i\eta} = \left[1 - \frac{1}{\mathcal{L} + \epsilon_k + i\eta}\left(\mathcal{L}_1 + \mathcal{L}_2\right)\right] \frac{1}{\mathcal{L}_0 + \epsilon_k + i\eta} \tag{A7}$$

in combination with

$$\left(\mathcal{L}_0 + \epsilon_k + i\eta\right) a_k^\dagger = i\eta a_k^\dagger, \tag{A8}$$

$$\mathcal{L}_1 a_k^\dagger = 0, \tag{A9}$$

and

$$\mathcal{L}_2 a_k^\dagger = -\lambda\xi_k(b^\dagger + b), \tag{A10}$$

Eq. (A3) is recast in the form

$$\alpha_k^\dagger = a_k^\dagger + \lambda\xi_k \frac{1}{\mathcal{L} + \epsilon_k + i\eta}\big(b^\dagger + b\big). \tag{A11}$$

Equation (A11) features two unknown quantities,

$$A_k = \frac{1}{\mathcal{L} + \epsilon_k + i\eta} b^\dagger \quad \text{and} \quad B_k = \frac{1}{\mathcal{L} + \epsilon_k + i\eta} b. \tag{A12}$$

Our next goal is to explicitly compute these two operators by expressing them as the solution of two coupled linear equations. Once at hand, the scattering-state operator is simply given by $\alpha_k^\dagger = a_k^\dagger + \lambda\xi_k(A_k + B_k)$.

To find A_k and B_k we resort once again to the operator identity of Eq. (A7). Carrying out the relevant commutators one obtains the pair of equations

$$(\epsilon_k - \omega_0 + i\eta)A_k = b^\dagger + \lambda \sum_{q>0} \xi_q \frac{1}{\mathcal{L} + \epsilon_k + i\eta}(a_q^\dagger + a_q), \tag{A13}$$

$$(\epsilon_k + \omega_0 + i\eta)B_k = b - \lambda \sum_{q>0} \xi_q \frac{1}{\mathcal{L} + \epsilon_k + i\eta}(a_q^\dagger + a_q). \tag{A14}$$

Applying yet again the operator identity of Eq. (A7) to the right-most term in Eqs. (A13) and (A14) one arrives at

$$(\epsilon_k - \omega_0 + i\eta)A_k = b^\dagger + \Sigma(\epsilon_k + i\eta)(A_k + B_k) + C_k, \tag{A15}$$

$$(\epsilon_k + \omega_0 + i\eta)B_k = b - \Sigma(\epsilon_k + i\eta)(A_k + B_k) - C_k, \tag{A16}$$

where

$$\Sigma(z) = \lambda^2 \sum_{q>0} \xi_q^2 \left(\frac{1}{z - \epsilon_q} - \frac{1}{z + \epsilon_q} \right) \tag{A17}$$

is the phononic self-energy and C_k equals

$$C_k = \lambda \sum_{q>0} \xi_q \left(\frac{a_q^\dagger}{\epsilon_k - \epsilon_q + i\eta} - \frac{a_q}{\epsilon_k + \epsilon_q + i\eta} \right). \tag{A18}$$

Here in deriving Eqs. (A15) and (A16) we made use of the fact that

$$\frac{1}{\mathcal{L}_0 + \epsilon_k + i\eta} \begin{pmatrix} a_q^\dagger \\ a_q \end{pmatrix} = \frac{1}{\epsilon_k \mp \epsilon_q + i\eta} \begin{pmatrix} a_q^\dagger \\ a_q \end{pmatrix}. \tag{A19}$$

Finally, introducing the 2×2 phononic Green function

$$\hat{G}(z) = \begin{bmatrix} z - \omega_0 - \Sigma(z) & -\Sigma(z) \\ -\Sigma(z) & -z - \omega_0 - \Sigma(z) \end{bmatrix}^{-1}, \tag{A20}$$

Eqs. (A15) and (A16) are rewritten in the compact form

$$\sigma_z \hat{G}^{-1}(\epsilon_k + i\eta) \begin{pmatrix} A_k \\ B_k \end{pmatrix} = \begin{pmatrix} b^\dagger + C_k \\ b - C_k \end{pmatrix}, \tag{A21}$$

whose solution is

$$\begin{pmatrix} A_k \\ B_k \end{pmatrix} = \hat{G}(\epsilon_k + i\eta)\sigma_z \begin{pmatrix} b^\dagger + C_k \\ b - C_k \end{pmatrix}. \tag{A22}$$

Here σ_z is the Pauli matrix. The scattering-state operators specified in Eq. (26) are obtained by combining Eqs. (A11), (A12), and (A22). Note that the function $g(z)$ defined in Eq. (27) is simply minus the determinant of $\hat{G}^{-1}(z)$.

2. Extension to nonzero ϵ_d

The case of a level off-resonance with the Fermi energy can, in principle, be treated using the same machinery as the one employed for $\epsilon_d = 0$. We, however, shall present a more concise derivation that makes use of the scattering-state operators obtained for $\epsilon_d = 0$. As in the main text, the notation $\alpha_k^\dagger$ will be reserved for the scattering-state operators when $\epsilon_d = 0$ while the new operators for $\epsilon_d \neq 0$ are denoted by $\beta_k^\dagger$.

Our starting point is the formal solution

$$\beta_k^\dagger = \frac{i\eta}{\mathcal{L} + \epsilon_k + i\eta} a_k^\dagger, \tag{A23}$$

where $\mathcal{L}$ pertains this time to the full Hamiltonian of Eq. (23) with $\tilde{\epsilon}_d \neq 0$. Using the notations of Eqs. (A4)–(A6), we divide the full Hamiltonian into two parts: $\mathcal{H}_{\epsilon_d=0} = \mathcal{H}_0 + \mathcal{H}_1 + \mathcal{H}_2$ and

$$\mathcal{H}_{\epsilon_d} = \tilde{\epsilon}_d \sum_{q>0} \xi_q \left(a_q + a_q^\dagger \right). \tag{A24}$$

Denoting the corresponding Liouville operators by $\mathcal{L}_{\epsilon_d=0}$ and $\mathcal{L}_{\epsilon_d}$, respectively, we employ the operator identity

$$\frac{1}{\mathcal{L} + \epsilon_k + i\eta} = \left[1 - \frac{1}{\mathcal{L} + \epsilon_k + i\eta} \mathcal{L}_{\epsilon_d} \right] \frac{1}{\mathcal{L}_{\epsilon_d=0} + \epsilon_k + i\eta} \tag{A25}$$

to rewrite Eq. (A24) in the form

$$\beta_k^\dagger = \left[1 - \frac{1}{\mathcal{L} + \epsilon_k + i\eta} \mathcal{L}_{\epsilon_d} \right] \frac{i\eta}{\mathcal{L}_{\epsilon_d=0} + \epsilon_k + i\eta} a_k^\dagger. \tag{A26}$$

Recognizing that

$$\frac{i\eta}{\mathcal{L}_{\epsilon_d=0} + \epsilon_k + i\eta} a_k^\dagger = \alpha_k^\dagger, \tag{A27}$$

we thus arrive at

$$\beta_k^\dagger = \alpha_k^\dagger - \frac{1}{\mathcal{L} + \epsilon_k + i\eta} \mathcal{L}_{\epsilon_d} \alpha_k^\dagger. \tag{A28}$$

Since $\alpha_k^\dagger$ and $\mathcal{H}_{\epsilon_d}$ are both linear in the original bosonic degrees of freedom, their commutator is a simple c-number:

$$\begin{aligned} \mathcal{L}_{\epsilon_d} \alpha_k^\dagger &= -\tilde{\epsilon}_d \xi_k \left[1 + g(\epsilon_k + i\eta) 2\omega_0 \Sigma(\epsilon_k + i\eta) \right] \\ &= -\tilde{\epsilon}_d \xi_k g(\epsilon_k + i\eta) \left(\epsilon_k^2 - \omega_0^2 \right). \end{aligned} \tag{A29}$$

Consequently, using Eq. (A28),

$$\beta_k^\dagger = \alpha_k^\dagger + \tilde{\epsilon}_d \xi_k \frac{\epsilon_k^2 - \omega_0^2}{\epsilon_k + i\eta} g(\epsilon_k + i\eta), \tag{A30}$$

which is precisely Eq. (36).

3. Change in frequency from ω_0 to $\omega_1 = \omega_0 + \delta\omega$

Lastly, we wish to expand the scattering-state operators $\gamma_k^\dagger$ corresponding to the Hamiltonian $\mathcal{H}' = \mathcal{H} + \delta\mathcal{H}$ in terms of those corresponding to $\mathcal{H}$ alone (i.e., the α_k's and $\alpha_k^\dagger$'s derived in Sec. A 1). Here $\mathcal{H}$ is the full Hamiltonian of Eq. (23) with $\tilde{\epsilon}_d = 0$ and $\delta\mathcal{H}$ equals

$$\delta\mathcal{H} = \delta\omega b^\dagger b. \tag{A31}$$

As in the previous subsection, we begin from the formal solution

$$\gamma_k^\dagger = \frac{i\eta}{\mathcal{L}' + \epsilon_k + i\eta} a_k^\dagger, \tag{A32}$$

where $\mathcal{L}'$ is the Liouville operator associated with $\mathcal{H}'$. Denoting the Liouville operators corresponding to $\mathcal{H}$ and $\delta\mathcal{H}$ by $\mathcal{L}$ and $\mathcal{L}_{\delta\omega}$, respectively, we make use of the operator identity

$$\frac{1}{\mathcal{L}' + \epsilon_k + i\eta} = \left[1 - \frac{1}{\mathcal{L}' + \epsilon_k + i\eta}\mathcal{L}_{\delta\omega}\right] \frac{1}{\mathcal{L} + \epsilon_k + i\eta} \tag{A33}$$

to rewrite Eq. (A32) in the form

$$\gamma_k^\dagger = \left[1 - \frac{1}{\mathcal{L}' + \epsilon_k + i\eta}\mathcal{L}_{\delta\omega}\right] \frac{i\eta}{\mathcal{L} + \epsilon_k + i\eta} a_k^\dagger. \tag{A34}$$

Recognizing once again that

$$\frac{i\eta}{\mathcal{L} + \epsilon_k + i\eta} a_k^\dagger = \alpha_k^\dagger, \tag{A35}$$

we arrive at

$$\gamma_k^\dagger = \alpha_k^\dagger - \frac{1}{\mathcal{L}' + \epsilon_k + i\eta}\mathcal{L}_{\delta\omega}\alpha_k^\dagger, \tag{A36}$$

which is analogous to Eq. (A28) of the previous subsection.

It is straightforward to confirm that Eq. (A36) is equivalent to the modified Lippmann-Schwinger equation

$$[\gamma_k^\dagger, \mathcal{H}'] = -\epsilon_k \gamma_k^\dagger + i\eta(\alpha_k^\dagger - \gamma_k^\dagger). \tag{A37}$$

Its usefulness stems from the fact that it allows one to directly expand $\gamma_k^\dagger$ in terms of the α_q's and $\alpha_q^\dagger$'s without resorting to the separate expansions of $\gamma_k^\dagger$ and $\alpha_k^\dagger$ in terms of the original bosonic degrees of freedom. Indeed, using Eq. (32) and its Hermitian conjugate one has that

$$\mathcal{L}_{\delta\omega}\alpha_k^\dagger = \delta\omega\lambda\xi_k g(\epsilon_k + i\eta)\left[(\epsilon_k - \omega_0)b - (\epsilon_k + \omega_0)b^\dagger\right], \tag{A38}$$

such that

$$\gamma_k^\dagger = \alpha_k^\dagger + \delta\omega\lambda\xi_k g(\epsilon_k + i\eta)\left[\epsilon_k A_k' + \omega_0 B_k'\right] \tag{A39}$$

with

$$A_k' = \frac{1}{\mathcal{L}' + \epsilon_k + i\eta}\left(b^\dagger - b\right) \tag{A40}$$

and

$$B_k' = \frac{1}{\mathcal{L}' + \epsilon_k + i\eta}\left(b^\dagger + b\right). \tag{A41}$$

Similar to the derivation in Sec. A 1, A_k' and B_k' are computed by expressing them as the solution of two coupled linear equations, obtained by applying the operator identity of Eq. (A33) to each of Eqs. (A40) and (A41). After some lengthy but straightforward algebra one obtains

$$\hat{M}(\epsilon_k + i\eta)\begin{pmatrix} A_k' \\ B_k' \end{pmatrix} = \begin{pmatrix} \mu_k \\ \nu_k \end{pmatrix}, \tag{A42}$$

with

$$\hat{M}(z) = \begin{bmatrix} 1 - \frac{\delta\omega}{\omega_0}\left(z^2 g(z) - 1\right) & -\delta\omega z g(z) \\ -\delta\omega z g(z) & 1 - \delta\omega\omega_0 g(z) \end{bmatrix}, \tag{A43}$$

$$\mu_k = 2\lambda\sum_{q>0}\xi_q\epsilon_q\left[\frac{g(\epsilon_q - i\eta)}{\epsilon_k - \epsilon_q + i\eta}\alpha_q^\dagger - \frac{g(\epsilon_q + i\eta)}{\epsilon_k + \epsilon_q + i\eta}\alpha_q\right], \tag{A44}$$

and

$$\nu_k = 2\omega_0\lambda\sum_{q>0}\xi_q\left[\frac{g(\epsilon_q - i\eta)}{\epsilon_k - \epsilon_q + i\eta}\alpha_q^\dagger + \frac{g(\epsilon_q + i\eta)}{\epsilon_k + \epsilon_q + i\eta}\alpha_q\right]. \tag{A45}$$

Inverting the matrix $\hat{M}(\epsilon_k + i\eta)$ to extract A_k' and B_k' and substituting the resulting expressions into Eq. (A39), one recovers Eq. (86) for $\gamma_k^\dagger$.

[1] L. Perfetti, P. A. Loukakos, M. Lisowski, U. Bovensiepen, H. Berger, S. Biermann, P. S. Cornaglia, A. Georges, and M. Wolf, Phys. Rev. Lett. **97**, 067402 (2006).

[2] F. Schmitt, P. S. Kirchmann, U. Bovensiepen, R. G. Moore, L. Rettig, M. Krenz, J.-H. Chu, N. Ru, L. Perfetti, D. H. Lu, M. Wolf, I. R. Fisher, and Z.-X. Shen, Science **321**, 1649 (2008).

[3] M. Greiner, O. Mandel, T. W. Hänsch, and I. Bloch, Nature **419**, 51 (2002).

[4] T. Kinoshita, T. Wenger, and D. S. Weiss, Nature **440**, 900 (2006).

[5] J. M. Elzerman, R. Hanson, L. H. W. van Beveren, B. Witkamp, L. M. K. Vandersypen, and L. P. Kouwenhoven, Nature **430**, 431 (2004).

[6] J. R. Petta, A. C. Johnson, J. M. Taylor, E. A. Laird, A. Yacoby, M. D. Lukin, C. M. Marcus, M. P. Hanson, and A. C. Gossard, Science **309**, 2180 (2005).

[7] P. Schmitteckert, Phys. Rev. B **70**, 121302 (2004); A.

Branschaedel, G. Schneider, and P. Schmitteckert, Ann. Phys. **522**, 657 (2010).
[8] K. A. Al-Hassanieh, A. E. Feiguin, J. A. Riera, C. A. Büsser, and E. Dagotto, Phys. Rev. B **73**, 195304 (2006); F. Heidrich-Meisner, A. E. Feiguin, and E. Dagotto, Phys. Rev. B **79**, 235336 (2009).
[9] F. B. Anders and A. Schiller, Phys. Rev. Lett. **95**, 196801 (2005).
[10] F. B. Anders and A. Schiller, Phys. Rev. B **74**, 245113 (2006).
[11] L. Mühlbacher and E. Rabani, Phys. Rev. Lett. **100**, 176403 (2008).
[12] S. Weiss, J. Eckel, M. Thorwart, and R. Egger, Phys. Rev. B **77**, 1953 (2008).
[13] P. Werner, T. Oka, and A. J. Millis, Phys. Rev. B **79**, 035320 (2009); P. Werner, T. Oka, M. Eckstein, and A. J. Millis, Phys. Rev. B **81**, 035108 (2010).
[14] M. Schiró and M. Fabrizio, Phys. Rev. B **79**, 153302 (2009).
[15] A. Alvermann and H. Fehske, Phys. Rev. Lett. **102**, 150601 (2009).
[16] M. Pletyukhov, D. Schuricht, and H. Schoeller, Phys. Rev. Lett. **104**, 106801 (2010); S. Andergassen, M. Pletyukhov, D. Schuricht, H. Schoeller, and L. Borda, Phys. Rev. B **83**, 205103 (2011).
[17] C. Karrasch, S. Andergassen, M. Pletyukhov, D. Schuricht, L. Borda, V. Meden, and H. Schoeller, Europhys. Lett. **90**, 30003 (2010).
[18] A. Hackl and S. Kehrein, J. Phys. C **21**, 015601 (2009); A. Hackl, M. Vojta, and S. Kehrein, Phys. Rev. B **80**, 195117 (2009); P. Wang and S. Kehrein, Phys. Rev. B **82**, 125124 (2010).
[19] A. Schiller and S. Hershfield, Phys. Rev. Lett. **77**, 1821 (1996); Phys. Rev. B **62**, 16271 (2000).
[20] D. Lobaskin and S. Kehrein, Phys. Rev. B **71**, 193303 (2005); M. Heyl and S. Kehrein, Phys. Rev. B **81**, 144301 (2010).
[21] For recent reviews see, e.g., *Introducing Molecular Electronics*, edited by G. Cuniberti, G. Fagas, and K. Richter, Lecture Notes in Physics Vol. 680 (Springer, New York, 2005); M. Galperin, M. A. Ratner, and A. Nitzan, J. Phys.: Condens. Matter **19**, 103201 (2007).
[22] L. I. Glazman and M. Raikh, JETP Lett. **47**, 452 (1988).
[23] I. G. Lang and Yu. A. Firsov, Zh. Eksp. Teor. Fiz. **43**, 1843 (1962) [Sov. Phys. JETP **16**, 1301 (1963)].
[24] B. Dóra and A. Halbritter, Phys. Rev. B. **80**, 155402 (2009).
[25] B. Dóra, Phys. Rev. B. **75**, 245113 (2007).
[26] B. Dóra and M. Gulácsi, Phys. Rev. B. **78**, 165111 (2008).
[27] We employ units in which $\hbar = 1$.
[28] D. Sherrington and S. von Molnàr, Solid St. Comm. **16**, 1347 (1975).
[29] A similar construction was used by E. Lebanon, A. Schiller, and F. B. Anders, Phys. Rev. B **68**, 155301 (2003).
[30] J. Gadzuk, Phys. Rev. B **24**, 1651 (1981).
[31] E. Blaisten-Barojas and J. Gadzuk, J. Chem. Phys. **97**, 862 (1992).
[32] C. C. Yu and P. W. Anderson, Phys. Rev. B **29**, 6165 (1984).
[33] F. D. M. Haldane, J. Phys. C **14**, 2585 (1981).
[34] We have omitted here the contribution of the $k = 0$ mode of $\partial_x \phi(x)$, as it has no effect on our problem of interest.
[35] A. Schiller and S. Hershfield, Phys. Rev. B **58**, 14978 (1998).
[36] We cannot *a priori* rule out the possibility of an additional branch cut in the analytical continuation of $g^*(\epsilon + i\eta)$ to the upper half plane. Our numerical results are consistent, however, with an analysis based on isolated poles only.
[37] See, e.g., *Handbook of Mathematical Functions*, eds. M. Abramowitz and I. A. Stegun (Dover, New York, 1972), Chapter 5.
[38] E. Eidelstein, D. Goberman, and A. Schiller (unpublished).
[39] Indeed, it is straightforward to confirm that the right-hand side of Eq. (57) equals $\int_{-\infty}^{\infty} \mathrm{Im}\{G_{11}(\epsilon + i\eta)\} d\epsilon/\pi$, where $G_{11}(z) = \ll b, b^\dagger \gg_z$ is the corresponding component of the phonon Green function of Eq. (A20). The latter integral is nothing but the zero-temperature equilibrium phononic occupancy, averaged with respect to the full Hamiltonian of Eq. (23) with $\tilde{\epsilon}_d$ set to zero.
[40] V. Ambegaokar, Ann. Phys. (Leipzig) **16**, 319 (2007).
[41] In comparing the parameters Ω and τ_0 extracted from the different fits used throughout the paper, the figures quoted for the deviations are exclusively due to τ_0. Indeed, the frequency Ω agrees to within less than 0.01% between all fits used.
[42] B. Doyon and N. Andrei, Phys. Rev. B **73**, 245326 (2006).
[43] V. Sazonova, Y. Yaish, H. Üstünel, D. Roundy, T. A. Arias, and P. L. McEuen, Nature **431**, 284 (2004).
[44] This identity is established straightforwardly by a formal diagrammatic evaluation of $\langle b \rangle$.
[45] The inclusion of η does not affect the end result of the calculation since each of the numerators in Eq. (118) vanishes along with its denominator.
[46] Due to the terms multiplying $|g(\Omega + i\eta)|^2$, the amplitude of oscillations A_b is in fact peaked at a slightly lower frequency than ω.
[47] J. M. Elzerman, S. De Franceschi, D. Goldhaber-Gordon, W. G. van der Wiel, and L. P. Kouwenhoven, J. Low Temp. Phys. **118**, 375 (2000).
[48] A. Kogan, S. Amasha, and M. A. Kastner, Science **304**, 1293 (2004).